Supplementary Information

Syntheses and characterization data

Materials and general instrumentations

Solvents and reagents were obtained from commercial suppliers and used without further purification. If required, solvents were distilled prior to use. For simplicity, solvents and reagents are indicated as follows: acetonitrile (MeCN), diethyl ether (Et_2O), ethyl acetate (EtOAc), petroleum ether (PE), tetrahydrofuran (THF), triethylamine (TEA), sodium hydroxide (NaOH), hydrochloric acid (HCl), sodium sulfate (Na_2SO_4), hydrogen peroxide (H_2O_2). Thin-layer chromatography analyses were performed using pre-coated Supelco silica gel on TLC Al foils 0.2 mm and visualized by UV (254 nm), and/or $KMnO_4$ stain. NMR experiments were run on a Varian Gemini 400 MHz spectrometer (400.13 MHz for ^1H, and 100.62 MHz for ^{13}C), equipped with a BBI probe and Z-gradients. Spectra were acquired at 300 K, using deuterated chloroform ($CDCl_3$) or dimethyl sulfoxide (DMSO-d_6) as solvents. Chemical shifts for ^1H and ^{13}C spectra were recorded in parts per million using the residual non-deuterated solvent as the internal standard. The experiment 1D NOESY was performed with NOE DPFGSE pulse sequence at the mixing time of 1,5 seconds. Data are reported as follows: chemical shift (ppm), multiplicity (indicated as: bs, broad signal; s, singlet; d, doublet; t, triplet; q, quartet; p, quintet; sx, sextet; m, multiplet and combinations thereof), coupling constants (J) in Hertz (Hz) and integrated intensity. The IR-FT spectra were recorded on a Jasco FT/IR-4100. Compounds were named using the naming algorithm developed by CambridgeSoft Corporation and used in ChemBioDraw Ultra 15.0. UPLC–MS analyses were run on a Waters ACQUITY UPLC/MS system consisting of a QDa mass spectrometer equipped with an electrospray ionization interface and a 2489 UV/Vis detector.

*General procedure for preparation of dimethylbenzene-1,2-diols **3,4DMC**, **3,5DMC**, **3,6DMC** and **4,5DMC*** [1]

A solution of the appropriate dimethylphenol **a1-4** (12.2 mmol), anhydrous $MgCl_2$ (18.4 mmol) and TEA (36.8 mmol) in ACN (6 mL) was prepared and stirred under nitrogen atmosphere for 15 minutes. Then *p*-formaldehyde (36.8 mmol) was added dropwise. The reaction was heated to 100° C and stirred for 2.5 hours. After cooling to room temperature, the mixture was acidified with 1N HCl (12 mL) and extracted with Et_2O (10 mL x 3). The organic layers were combined and dried over anhydrous Na_2SO_4. The solvent was evaporated to obtain the corresponding crude intermediate aldehydes **b1-4** as yellow solid, which were used to the next step without further purification.

The aldehydes **b1-4** were dissolved in THF (5 mL) and H_2O (1 mL) and cooled to 0° C. Then 5M NaOH (2.4 mL) and 30% H_2O_2 (1.2 mL) were added dropwise and the reaction was stirred at room temperature for 30 minutes. The mixture was diluted with 2N HCl (12 mL) and extracted with Et_2O (10 mL x 3). The collected organic layers were dried over anhydrous Na_2SO_4 and the solvent was removed to provide the corresponding crude products, which were purified by flash silica gel chromatography (PE-EtOAc) to give the desired **3,4DMC**, **3,5DMC**, **3,6DMC** and **4,5DMC**.

3,4-dimethylbenzene-1,2-diol (**3,4DMC**)

2,3-dimethylphenol **a1** (1.5 g, 11.3 mmol) and *p*-formaldehyde (1.108 g, 36.9 mmol) were reacted to achieve the intermediate aldehyde **b1** which in turn was treated to give the crude product of **3,4DMC**, according to general procedure. The crude product was purified by flash silica gel chromatography (PE-EtOAc, gradient up to 88-12) to provide **3,4DMC** as pale-yellow solid (726 mg, yield 43%). The spectroscopic data are in agreement with those reported in literature [2]. ^1H NMR (400 MHz, DMSO-d_6) δ 6.48 (d, 1 H, J = 8 Hz, CH), 6.4 (d, 1 H, J = 8 Hz, CH), 8.4 (br, 2 H, OH, exchange with D_2O),

2.07 (s, 3 H, CH_3), 2.01 (s, 3 H, CH_3). ^{13}C NMR (100 MHz, $CDCl_3$) δ 142.18, 140.96, 129.97, 123.08, 121.04, 112.05, 19.44, 11.72 . IR (nujol) ν_{max} cm^{-1} 3478, 3364. ESI-MS for $C_8H_{10}O_2$: calculated 138.07, found m/z 137.09 $[M - H]^-$.

3,5-dimethylbenzene-1,2-diol (**3,5DMC**)

3,5-dimethylphenol **a2** (1.5 g, 11.3 mmol) and *p*-formaldehyde (1.10 g, 36.9 mmol) were reacted to achieve the intermediate aldehyde **b2** which in turn was treated to give the crude product of **3,5DMC**, according to general procedure. The crude product was purified by flash silica gel chromatography (PE-EtOAc, gradient up to 95-5) to provide **3,5DMC** as white solid (620 mg, yild 37%). The spectroscopic data agree with those reported in literature [3]. ^1H NMR (400 MHz, $CDCl_3$) δ 6.53 (s, 1H, CH), 6.51 (s, 1 H, CH), 4.99 (s, 1 H, OH, exchange with D_2O), 4.83 (s, 1 H, OH, exchange with D_2O), 2.21 (s, 3 H, CH_3), 2.20 (s, 3 H, CH_3). ^{13}C NMR (100 MHz, $CDCl_3$) δ 143.0, 139.7, 130.1, 124.4, 123.5, 123.4, 113.8, 113.7, 20.7, 15.5. IR (nujol) ν_{max} cm^{-1} 3430 (broad, OH), 3255 (broad, OH). ESI-MS for $C_8H_{10}O_2$: calculated 138.07, found m/z 137.09 $[M - H]^-$.

3,6-dimethylbenzene-1,2-diol (**3,6DMC**)

2,5-dimethylphenol **a3** (1.5 g, 11.3 mmol) and *p*-formaldehyde (1.104 g, 36.8 mmol) were reacted to achieve the intermediate aldehyde **b3** which in turn was treated to give the crude product of **3,6DMC**, according to general procedure [1]. The crude product was purified by flash silica gel chromatography (PE-EtOAc, gradient up to 93-7) to provide **3,6DMC** as white solid (315 mg, yield 19%). The spectroscopic data are in agreement with those reported in literature [2, 4]. ^1H NMR (400 MHz, $CDCl_3$) δ 6.62 (s, 2 H, CH), 5.02 (s, 2 H, OH, exchange with D_2O), 2.23 (s, 6 H, CH_3). ^{13}C NMR (100 MHz, $CDCl_3$) δ 141.8, 121.9, 121.7, 15.5. The molecular structure was confirmed by the ^1H-NMR NOE spectroscopy experiment through the irradiation of CH proton which yielded the enhancement of CH_3 protons signal. IR (nujol) ν_{max} cm^{-1} 3348 (broad, 2 x OH). ESI-MS for $C_8H_{10}O_2$: calculated 138.07, found m/z 137.09 $[M - H]^-$.

4,5-dimethylbenzene-1,2-diol (**4,5DMC**)

3,4-dimethylphenol **a4** (1.22 g, 10.0 mmol) and *p*-formaldehyde (901 mg, 30.0 mmol) were reacted to achieve the intermediate aldehyde **b4** which in turn was treated to give the crude product of **4,5DMC**, according to general procedure. The crude product was purified by flash silica gel chromatography (PE-EtOAc, gradient up to 88-12) to provide **4,5DMC** as white solid (420 mg, yield 30%). The spectroscopic data are in agreement with those reported in literature [2, 5]. ^1H NMR (400 MHz, $CDCl_3$) δ 6.65 (s, 2 H, CH), 4.83 (s, 2 H, OH, exchange with D_2O), 2.14 (s, 6 H, CH_3). ^{13}C NMR (100 MHz, $CDCl_3$) δ 141.2, 129.91, 117.0, 19.1. IR (nujol) ν_{max} cm^{-1} 3375 (broad, 2 x OH). ESI-MS for $C_8H_{10}O_2$: calculated 138.07, found m/z 137.19 $[M - H]^-$.

Protein crystallization

Aliquots of 11 mg mL^{-1} SPU, dissolved in 50 mM HEPES buffer at pH 7.5, also containing 50 mM Na_2SO_3 as a reducing agent, were subjected to successive dilution - concentration cycles using Amicon Ultra centrifugal filter units - MWCO 10 KDa (Merck Millipore) and 50 mM HEPES buffer at pH 7.5, in order to remove Na_2SO_3. After a final concentration step up to 2 mg mL^{-1}, each SPU solution was incubated in the presence of 0.5 mM **3MC**, 2.5 mM **4MC**, 1.0 mM **3,4DMC**, 0.5 mM **3,5DMC**, 1.0 mM **4,5DMC** and 1.0 mM **3,6DMC**, respectively, all dissolved in the same buffer. After a proper incubation period, during which the enzyme activity was abolished (approximately 1-3 hours, depending on the nature of derivative), SPU-inhibitor solutions were concentrated up to 11 mg mL^{-1} and crystallization drops were made by diluting 1.5 μL of SPU-inhibitor solution with 1.5

μL of a precipitant solution containing 1.6-2.1 M $(NH_4)_2SO_4$ dissolved in 100 mM sodium citrate buffer, at pH 6.3. No inhibitor was present in the precipitant solution, so that the crystallizations occurred in the presence of 0.25 mM **3MC**, 1.25 mM **4MC**, 0.5 mM **3,4DMC**, 0.25 mM **3,5DMC**, 0.5 mM **4,5DMC**, and 0.5 mM **3,6DMC**, respectively. Crystallization trials were performed at 293 K using the vapor diffusion technique (hanging-drop method), equilibrating the drop against 1 mL of the precipitant solution using 24-well XRL Plate (Molecular Dimensions, Suffolk, UK) Rice-shaped protein crystals (dimensions up to 0.1 x 0.1 x 0.3 mm^3) typically grew in the presence of 1.7-2.0 M $(NH_4)_2SO_4$ after 1-2 weeks. Crystals were cryoprotected by transferring them in a solution containing 100 mM citrate buffer at pH 6.3, 2.4 M $(NH_4)_2SO_4$, and 20% (v/v) ethylene glycol, and then flash-cooled and stored in liquid nitrogen.

Quantum mechanical calculations.

Density functional theory (DFT) computations were carried out using the program ORCA 4.1.0 [35] and the Becke three-parameter hybrid functional combined with Lee-Yang-Parr correlation functional [36] as defined in the Gaussian software [37] (B3LYP/G). In a first set of calculations, the conformational space of all the possible conformations of the semiquinones deriving from each of the catechol derivatives investigated in this work was investigated. Subsequently, the geometries of the reaction intermediates obtained in the second step of the reactions between the most stable conformations of the semiquinones considered in the first set of calculations and a model of αCys322(Sγ) consisting of a CH_3SH moiety [16i]. The geometry optimizations carried out on the previously described molecules were performed by using the Dunning correlation-consistent polarized triple zeta basis set, with the inclusion of diffuse functions, (aug-cc-pVTZ) [38] was used. Frequency computations were performed to determine the nature of the minimized structures. Finally, for each of the most stable intermediates of each catechol derivative, the dissociation of the bond between the carbon atom of the catechol derivative and the sulfur atom from the CH_3SH moiety was investigated using relaxed surface scan computations [35], which involve constrained optimizations for different values of a selected reaction coordinate. The chosen coordinate, in this case the bond distance, is fixed to a certain value while the remaining coordinates of the molecule are optimized. After completion of one optimization cycle, the value of the reaction coordinate is changed, and another optimization cycle is carried out. This procedure was used to trace a path (theoretically close to a minimum energy path) from the reaction intermediates to the separated catechol derivatives and the CH_3SH moiety in the radical form (methylsufanyl, $CH_3S\bullet$). For relaxed scan calculations all atoms were described by the Pople-style 6-311G(d,p) basis set [37].

Table 1-SI. Data collection, processing and refinement statistics for the crystal structures of SPU bound to **3MC**, **4MC**, **3,4DMC**, **3,5DMC**, **4,5DMC**, and **3,6DMC** (PDB codes 6ZNY, 6ZNZ, 6ZO0, 6ZO1, 6ZO2 and 6ZO3).

ligand (PDB code)	**3MC (6ZNY)**	**4MC (6ZNZ)**	**3,4DMC (6ZO0)**	**3,5DMC (6ZO1)**	**4,5DMC (6ZO2)**	**3,6DMC (6ZO3)**
Data collection						
Wavelength (Å)	0.9537	0.9537	1.0000	0.9660	0.9677	0.9677
Detector	DECTRIS PILATUS 6M	DECTRIS PILATUS 6M	DECTRIS PILATUS 6M	DECTRIS PILATUS 6M	EIGER X 4M	EIGER X 4M
Crystal-to-Detector distance (mm)	251.18	330.02	347,64	185.788	101.34	101.32
Oscillation angle (degrees)	0.100	0.100	0.500	0.100	0.100	0.100
Number of images	1400	400	200	800	1800	1400
Space group	$P6_322$	$P6_322$	$P6_322$	$P6_322$	$P6_322$	$P6_322$
Unit cell (*a*, *b*, *c*, Å)	131.6, 131.6, 189.4	131.0, 131.0, 188.9	131.5, 131.5, 188.7	131.6, 131.6, 188.9	131.6, 131.6, 189.3	131.5, 131.5, 189.1
Resolution range (Å)[a]	1.50-97.64 (1.50-1.53)	1.89-97.27 (1.89-1.93)	2.23-188.71 (2.23-2.30)	1.61-45.49 (1.61-1.64)	1.65-62.17 (1.65-1.68)	1.55-48.77 (1.55-1.58)
Total number of reflections[a]	2354825 (110984)	337321 (18598)	5100187 (47173)	1082265 (53467)	2379195 (120332)	2232515 (103736)
Unique reflections[a]	153039 (7425)	76691 (4494)	47585 (4300)	123908 (6001)	116041 (5665)	139215 (6635)
Multiplicity[a]	15.4 (14.9)	4.4 (4.1)	10.7 (11.0)	8.7 (8.9)	20.5 (21.2)	16.0 (15.6)
Completeness[a] (%)	99.7 (99.1)	99.8 (99.8)	100.0 (100.0)	99.8 (99.6)	100.0 (100.0)	99.9 (97.5)
R_{sym}[a,b] (%)	11.3 (235.9)	12.4 (84.2)	27.1 (175.1)	9.7 (165.9)	13.1 (281.1)	12.7 (214.5)
R_{pim}[a,c] (%)	3.0 (64.5)	7.5 (54.1)	9.1 (58.3)	3.7 (60.5)	3.0 (63.4)	3.4 (57.1)
Mean I half-set correlation CC(1/2)[a]	0.999 (0.687)	0.994 (0.675)	0.995 (0.657)	0.999 (0.610)	0.999 (0.771)	0.999 (0.670)
Mean I/σ(I)[a]	18.8 (1.5)	9.5 (1.5)	9.0 (1.5)	12.4 (1.5)	18.6 (1.5)	17.8 (1.5)
Number of monomers in the asymmetric unit	3	3	3	3	3	3
R_{factor}[d] (%)	13.3	15.9	16.11	13.57	13.44	13.55
R_{free}[d] (%)	15.2	17.8	21.62	15.90	15.56	15.60
Cruickshank's DPI for coordinate error[e] based on R_{factor} (Å)	0.050	0.121	0.223	0.062	0.066	0.056
Wilson plot B-factor (Å^2)	15.9	17.2	27.9	21.3	20.6	13.2
Average all atom B-factor[f] (Å^2)	23.45	27.64	34.62	26.90	27.52	22.42
B-factor[f] for the Ni atoms (Å^2)	19.2, 18.0	30.0, 26.8	37.5, 39.8	22.6, 21.5	23.4, 22.3	18.8, 17.7
RMS (bonds)[d]	0.011	0.011	0.011	0.012	0.012	0.012
RMS (angles)[d]	1.755	1.655	1.922	1.82	1.751	1.765
Total number of atoms	7185	7006	6778	7068	7073	7155
Total number of water molecules	717	585	372	567	649	759
Solvent content (%)	55.57	55.07	55.36	55.45	55.58	55.42
Matthews Coefficient (Å^3/Da)	2.77	2.74	2.75	2.76	2.77	2.76
Most favored regions (%)	90.5	90.4	88.5	90.7	90.4	90.0
Additionally allowed regions (%)	8.5	8.6	10.4	8.3	8.6	9.0
Generously allowed regions (%)	0.8	0.8	0.9	0.8	0.8	0.8
Disallowed regions (%)	0.2	0.2	0.2	0.2	0.2	0.2

[a] Highest resolution bin in parentheses;

[b] $R_{sym} = \sum_{hkl}\sum_{j}|I_j - \langle I\rangle| / \sum_{hkl}\sum_{j} I_j$, where I is the intensity of a reflection, and ⟨I⟩ is the mean intensity of all symmetry related reflections j; [c] $R_{p.i.m.} = \sum_{hkl}\{[1/(N-1)]^{1/2}\sum_{j}|I_j - \langle I\rangle|\} / \sum_{hkl}\sum_{j} I_j$, where I is the intensity of a reflection, and ⟨I⟩ is the mean intensity of all symmetry related reflections j, and N is the multiplicity [6];

[d] Taken from REFMAC [7]; R_{free} is calculated using 5% of the total reflections that were randomly selected and excluded from refinement;

[e] $DPI = R_{factor} \cdot D_{max} \cdot compl^{-1/3} \sqrt{\frac{N_{atoms}}{(N_{refl} - N_{params})}}$, where N_{atoms} is the number of the atoms included in the refinement, N_{refl} is the number of the reflections included in the refinement, D_{max} is the maximum resolution of reflections included in the refinement, *compl* is the completeness of the observed data, and for isotropic refinement, $N_{params} \approx 4N_{atoms}$ [8];

[f] Taken from BAVERAGE[9];

[g] Taken from PROCHECK[9].

Table 2-SI. Cα RMSD of the crystal structures of SPU bound to **3MC**, **4MC**, **3,4DMC**, **3,5DMC**, **4,5DMC**, and **3,6DMC** (PDB codes 6ZNY, 6ZNZ, 6ZO0, 6ZO1, 6ZO2 and 6ZO3) calculated with respect to the native (PDB code 4CEU)[10] and catechol-bound SPU (PDB code 5G4H). All values are reported in Å.

ligand (PDB code)	**3MC (6ZNY)**		**4MC (6ZNZ)**		**3,4DMC (6ZO0)**		**3,5DMC (6ZO1)**		**4,5DMC (6ZO2)**		**3,6DMC (6ZO3)**	
	(4CEU) NAT	**(5G4H) CAT**	**(4CEU) NAT**	**(5G4H) CAT**	**(4CEU) NAT**	**(5G4H) CAT**	**(4CEU) NAT**	**(5G4H) CAT**	**(4CEU) NAT**	**(5G4H) CAT**	**(4CEU) NAT**	**(5G4H) CAT**
α	0.095	0.080	0.090	0.080	0.171	0.151	0.116	0.103	0.094	0.080	0.069	0.077
β	0.109	0.069	0.099	0.069	0.198	0.167	0.134	0.090	0.117	0.073	0.106	0.062
γ	0.122	0.079	0.117	0.074	0.176	0.139	0.137	0.083	0.130	0.078	0.113	0.069

Table 3-SI. Selected distances and angles around the Ni(II) ions in the crystal structures of SPU bound to **3MC**, **4MC**, **3,4DMC**, **3,5DMC**, **4,5DMC**, and **3,6DMC** (PDB codes 6ZNY, 6ZNZ, 6ZO0, 6ZO1, 6ZO2 and 6ZO3). The same distances and angles measured in the structure of SPU in the native state (PDB code 4CEU)[10] and bound to **CAT** (PDB code 5G4H)[11] are reported as a comparison.

(PDB code) ligand	**(6ZNY) 3MC**	**(6ZNZ) 4MC**	**(6ZO0) 3,4DMC**	**(6ZO1) 3,5DMC**	**(6ZO2) 4,5DMC**	**(6ZO3) 3,6DMC**	**(5G4H) CAT[11]**	**(4CEU) NAT[10]**
Ni - L Distances (Å) [(a)]								
Ni(1) - αLys220* Oθ1	2.0	2.1	1.9	2.0	2.0	2.0	2.0	1.9
Ni(1) - L_B	2.1	2.0	2.0	2.1	2.1	2.1	1.9	2.1
Ni(1) - L_1	2.1	2.3	2.4	2.2	2.2	2.2	2.2	2.2
Ni(1) - αHis249 Nδ	2.0	2.0	2.1	2.0	2.0	2.0	2.0	2.0
Ni(1) - αHis275 Nε	2.0	2.1	2.1	2.0	2.0	2.0	2.1	2.0
Ni(2) - αLys220* Oθ2	2.1	2.1	2.2	2.1	2.1	2.1	2.1	2.1
Ni(2) - L_B	2.1	2.1	2.3	2.1	2.1	2.1	2.0	2.1
Ni(2) - L_2	2.2	2.4	2.3	2.2	2.2	2.1	2.2	2.1
Ni(2) - αHis137 Nε	2.1	2.1	2.1	2.1	2.1	2.1	2.1	2.1
Ni(2) - αHis139 Nε	2.1	2.1	2.2	2.1	2.1	2.1	2.1	2.1
Ni(2) - αAsp363 Oδ1	2.1	2.2	2.3	2.1	2.1	2.1	2.1	2.1
Ni(1) ••• Ni(2)	3.7	3.6	3.8	3.7	3.7	3.7	3.6	3.7
L_1 ••• L_2	2.3	2.0	2.1	2.2	2.2	2.2	2.3	2.4
L - Ni - L Angles (°)								
αLys220* Oθ1 - Ni(1) - αHis249 Nδ	100.5	105.5	109.5	102.4	102.5	101.7	101.3	100.4
αLys220* Oθ1 - Ni(1) - αHis275 Nε	104.3	108.8	109.7	103.0	103.6	105.5	107.2	107.2
αLys220* Oθ1 - Ni(1) - L_B	96.8	96.7	100.9	96.3	97.1	94.9	89.9	96.6
αLys220* Oθ1 - Ni(1) - L_1	108.3	108.7	102.6	108.6	107.5	107.1	107.9	108.2
αHis249 Nδ - Ni(1) - αHis275 Nε	99.3	92.5	91.1	97.9	96.2	97.0	95.3	98.6
αHis275 Nε - Ni(1) - L_B	98.0	100.1	102.1	97.2	98.2	100.3	101.9	94.6
L_B - Ni(1) - L_1	63.0	63.5	61.1	62.0	63.9	61.0	70.1	67.0
L_1 - Ni(1) - αHis249 Nδ	90.1	89.2	94.2	92.8	91.2	92.1	85.8	89.3
αHis249 Nδ - Ni(1) - L_B	151.6	149.4	140.6	152.6	152.2	151.8	155.7	154.2
αHis275 Nε - Ni(1) - L_1	143.8	140.5	143.3	143.4	145.5	143.5	143.9	141.6
αLys220* Oθ2 - Ni(2) - αHis137 Nε	92.3	95.4	97.4	92.5	92.3	91.7	92.1	90.8
αLys220* Oθ2 - Ni(2) - αHis139 Nε	91.4	89.7	91.0	91.9	92.2	91.7	92.6	91.7
αLys220* Oθ2 - Ni(2) - L_2	92.3	90.2	93.2	92.0	91.6	92.0	93.3	92.9
αLys220* Oθ2 - Ni(2) - L_B	95.0	94.8	91.5	96.3	95.6	93.2	90.2	95.6
αAsp363 Oδ1 - Ni(2) - αHis137 Nε	83.1	81.8	83.1	83.7	83.7	83.2	81.6	82.8
αAsp363 Oδ1 - Ni(2) - αHis139 Nε	85.6	86.5	81.4	86.6	85.9	86.2	84.3	86.4
αAsp363 Oδ1 - Ni(2) - L_2	93.7	94.4	88.4	92.6	93.3	94.4	94.5	94.5
αAsp363 Oδ1 - Ni(2) - L_B	90.3	90.8	91.5	87.3	88.4	91.6	96.0	89.1
L_2 - Ni(2) – L_B	62.4	63.8	63.1	63.5	62.5	60.6	69.9	67.7
L_B - Ni(2) - αHis137 Nε	97.2	95.1	101.1	97.6	97.2	97.3	91.7	95.0
αHis137 Nε- Ni(2) - αHis139 Nε	109.4	113.0	111.4	109.1	109.1	109.8	112.2	108.5
αHis139 Nε- Ni(2) - L_2	90.6	87.7	82.9	89.2	90.7	92.0	85.9	88.4
αLys220* Oθ2 - Ni(2) - αAsp363 Oδ1	173.3	173.9	171.9	175.1	174.7	173.4	171.3	172.4
L_B - Ni(2) - αHis139 Nε	152.4	151.1	145.5	150.7	152.3	152.3	155.8	155.3
L_2- Ni(2) - αHis137 Nε	159.4	158.6	162.0	151.7	159.6	157.8	160.8	162.6
Ni(1) - L_B - Ni(2)	121.5	122.5	112.2	119.4	120.2	124.6	135.1	122.1

[(a)] L_1, L_2 indicate the ligand atom bound to Ni(1) and Ni(2), respectively, while L_B indicates the Ni-bridging ligand atom.

Table 4-SI. Selected distances and angles around the catechol derivatives in the crystal structures of SPU bound to **3MC**, **4MC**, **3,4DMC**, **3,5DMC**, **4,5DMC**, and **3,6DMC** (PDB codes 6ZNY, 6ZNZ, 6ZO0, 6ZO1, 6ZO2 and 6ZO3). The same distances and angles measured in the structure of SPU bound to **CAT** (PDB code 5G4H) [11] are reported as a comparison. Atom numbering follows that reported in **Schemes 1-6-SI**. In the **distances** field, the values corresponding to the distance between αCys322 Sγ and the bonded aromatic carbon atom are represented in bold. The same carbon atom, as well as the aromatic carbon atoms directly bonded to it, are renamed C_{aro}, C_{aro+1} and C_{aro-1}, respectively, in the **angles and torsion angles** field.

(PDB code) ligand	**(6ZNY) 3MC**	**(6ZNZ) 4MC**	**(6ZO0) 34DMC**	**(6ZO1) 35DMC**	**(6ZO2) 45DMC**	**(6ZO3) 36DMC**	**(5G4H) CAT[11]**
Distances (Å)							
C1 - αCys322 Sγ	2.7	4.0	2.7	2.7	3.9	4.5	4.0
C2 - αCys322 Sγ	4.0	2.7	4.0	4.0	2.7	4.0	2.6
C3 - αCys322 Sγ	4.5	**1.7**	4.6	4.5	**1.7**	2.7	**1.6**
C4 - αCys322 Sγ	4.0	2.7	4.0	4.0	2.7	**1.7**	2.7
C5 - αCys322 Sγ	2.7	4.0	2.7	2.7	4.0	2.6	4.0
C6 - αCys322 Sγ	**1.7**	4.5	**1.7**	**1.7**	4.5	4.0	4.5
O1 - αCys322 Sγ	3.0	5.1	3.1	2.9	5.0	5.8	5.0
O2 - αCys322 Sγ	5.1	2.9	5.0	5.0	2.9	5.1	2.8
C_{M3} - αCys322 Sγ	6.0	---	6.1	6.0	---	3.1	----
C_{M4} - αCys322 Sγ	---	3.2	5.2	---	3.0	---	---
C_{M5} - αCys322 Sγ	---	---	---	3.1	5.2	---	---
C_{M6} - αCys322 Sγ	---	---	---	---	---	5.1	---
Angles and torsion angles (°)							
αCys322 Cβ - αCys322 Sγ – C_{aro}	100.4	106.7	114.7	101.3	104.0	97.6	108.3
αCys322 Sγ - C_{aro} - C_{aro+1}	120.1	123.0	121.6	117.7	120.4	117.6	125.2
αCys322 Sγ - C_{aro} - C_{aro-1}	119.4	117.9	120.2	123.1	118.3	122.8	115.8
αCys322 Cβ - αCys322 Sγ - C_{aro} - C_{aro+1}	-68.3	112.6	-92.0	-69.9	107.2	-69.9	108.9
αCys322 Cβ - αCys322 Sγ - C_{aro} - C_{aro-1}	113.4	-64.8	88.3	109.8	-71.0	110.4	-69.4

Table 5-SI. Kinetic parameters for inhibition of JBU by the mono- and di-substituted catechol derivatives tested at 20 μM. The same data determined for CAT[11] are shown as a comparison.

Compound	k_1 x 10^4 (s^{-2})	k_2 x 10^6 (s^{-1})	k_1 x k_2 x 10^{10} (s^{-3})
CAT	0.72	5.87	4.23
3MC	13.18	6.11	80.53
4MC	1.53	3.17	4.85
3,4DMC	16.52	2.61	43.11
3,5DMC	3.80	0.31	1.18
4,5DMC	12.14	3.94	47.83
3,6DMC	2.17	0.33	0.72

Table 6-SI. Possible conformations of 3-methyl-semiquinone optimized at the B3LYP/G aug-cc-pVTZ level. For each conformer, the name, the formation energy (Hartrees) and the spin density are reported. The energy difference in kcal mol^{-1} with respect to the most stable conformation is reported into square brackets.

3MS_1: -421.544894 [1.94] 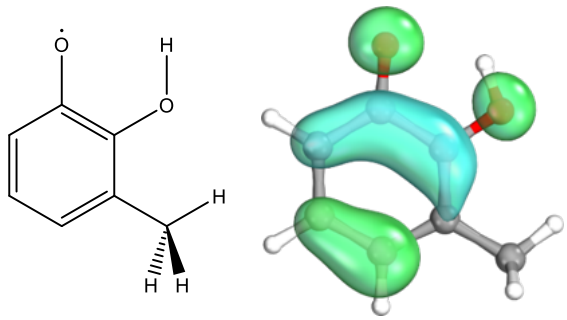	3MS_5: -421.546038 [1.22] 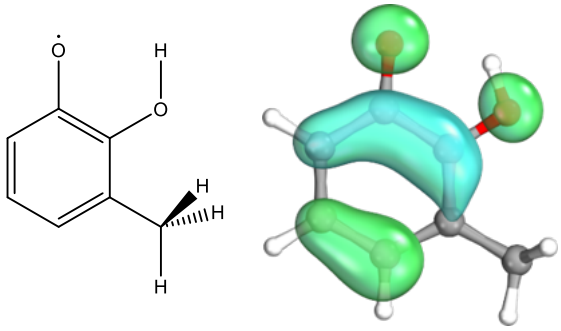
3MS_2: -421.528536 [12.20] 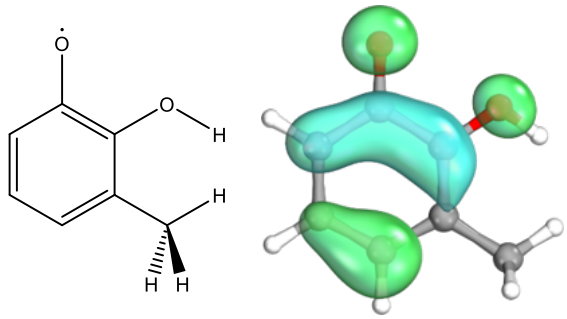	3MS_6: -421.530752 [10.81] 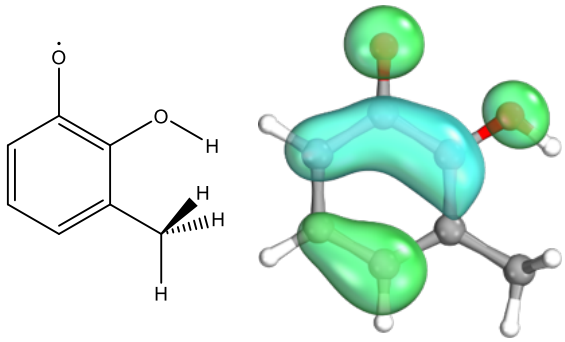
3MS_3: -421.532476 [9.73] 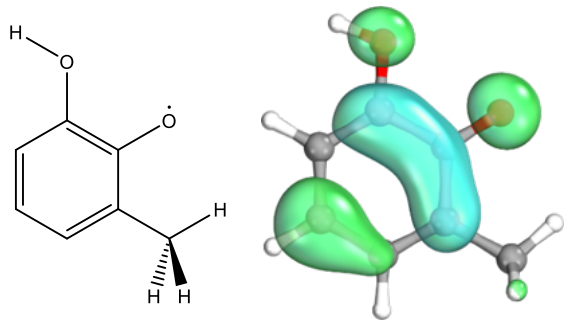	3MS_7: -421.533852 [8.87] 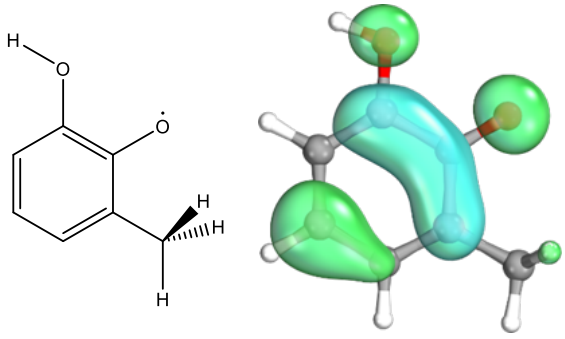
3MS_4: -421.546623 [0.85] 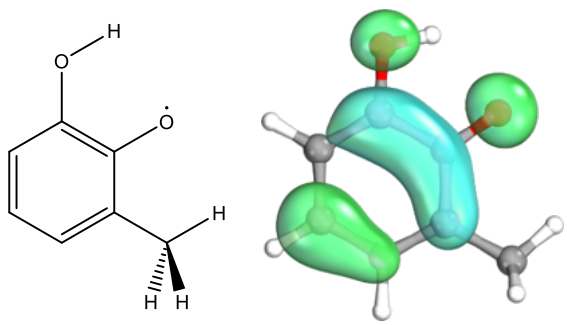	3MS_8: -421.547984 [0.00]* 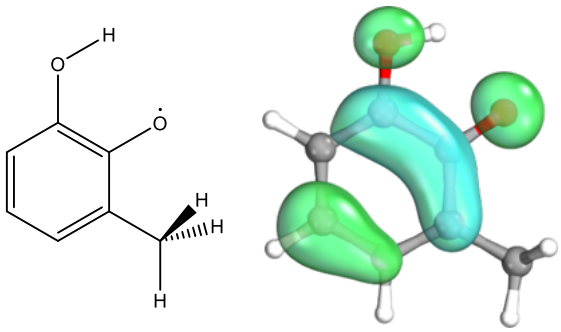

* Most stable conformation.

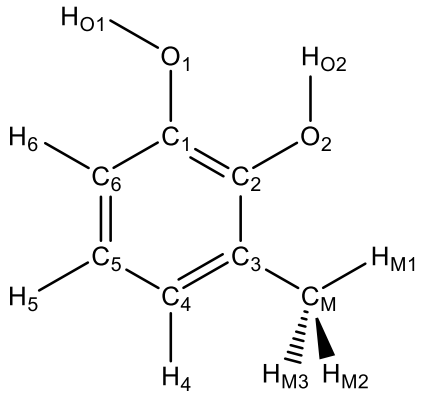

Scheme 1-SI. 3-metyl-catechol atoms numeration scheme.

Table 7-SI. B3LYP/G aug-cc-pVTZ spin density fraction on 3-methyl-semiquinone atoms. Atoms are named accordingly to Scheme 1-SI. The most stable conformation has been indicated with an asterisk, while the atom bearing the larger spin density fraction of each conformation has been highlighted in bold.

	Conformation							
Atom	**3MS_1**	**3MS_2**	**3MS_3**	**3MS_4**	**3MS_5**	**3MS_6**	**3MS_7**	**3MS_8***
C_1	0.079	0.046	0.180	0.181	0.080	0.047	0.188	0.186
C_2	0.191	0.186	0.059	0.090	0.202	0.198	0.059	0.090
C_3	-0.028	-0.033	0.160	0.133	-0.025	-0.031	0.150	0.125
C_4	0.214	0.229	-0.022	-0.001	0.203	0.218	-0.018	0.002
C_5	0.015	-0.012	0.214	0.206	0.017	-0.009	0.220	0.210
C_6	0.124	0.158	-0.036	-0.032	0.113	0.145	-0.036	-0.032
O_1	**0.298**	**0.332**	0.073	0.083	**0.300**	**0.335**	0.076	0.086
O_2	0.088	0.077	**0.333**	**0.305**	0.093	0.082	**0.323**	**0.296**
C_M	-0.003	-0.003	0.009	0.007	-0.003	-0.003	0.009	0.007
H_{O1}	-	-	0.003	0.005	-	-	0.003	0.005
H_{O2}	0.005	0.003	-	-	0.005	0.003	-	-
H_4	0.016	0.017	-0.002	0.000	0.015	0.017	-0.002	0.000
H_5	0.001	-0.001	0.016	0.015	0.001	-0.001	0.016	0.015
H_6	0.006	0.008	-0.004	-0.004	0.005	0.007	-0.004	-0.004
H_{M1}	0.000	-0.001	0.001	0.000	0.000	0.000	0.000	0.000
H_{M2}	-0.003	-0.003	0.008	0.006	-0.003	-0.004	0.008	0.007
H_{M3}	-0.003	-0.003	0.008	0.006	-0.003	-0.004	0.008	0.007
Total	1.000	1.000	1.000	1.000	1.000	1.000	1.000	1.000

Table 8-SI. Possible conformations of 4-methyl-semiquinone optimized at the B3LYP/G aug-cc-pVTZ level. For each conformer, the name, the formation energy (Hartrees) and the spin density are reported. The energy difference in kcal mol^{-1} with respect to the most stable conformation is reported into square brackets.

4MS_1: -421.547235 [0.00]* 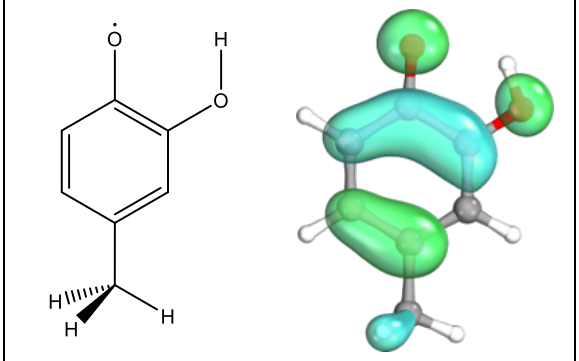	4MS_5: -421.546777 [0.29] 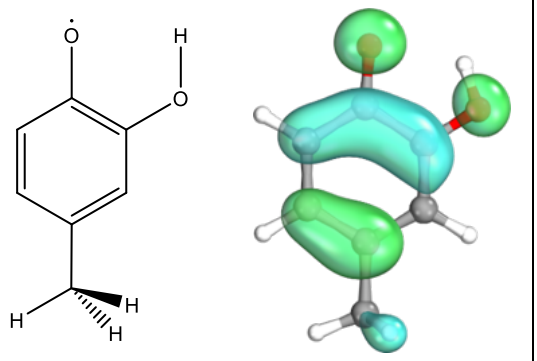
4MS_2: -421.532770 [9.08] 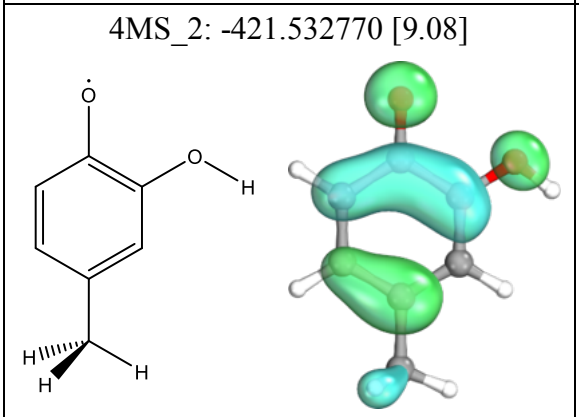	4MS_6: -421.532449 [9.28] 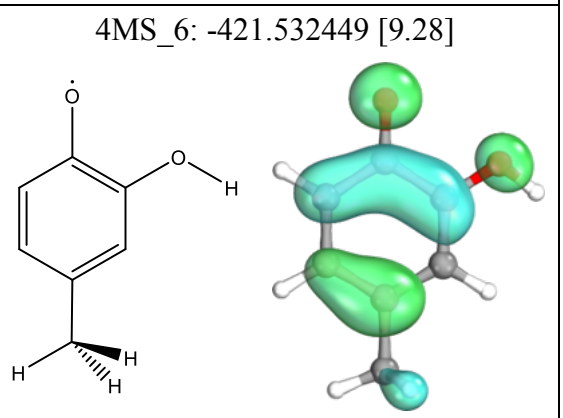
4MS_3: -421.531384 [9.95] 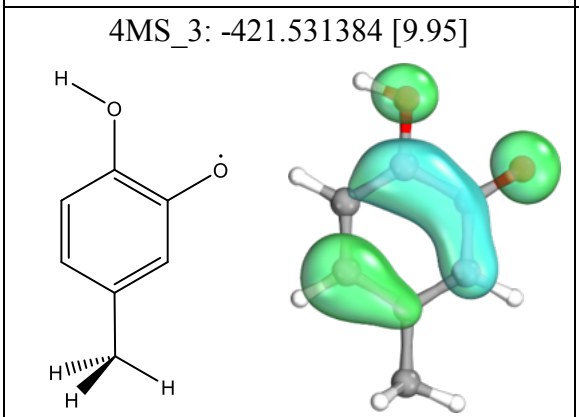	4MS_7: -421.530479 [10.51] 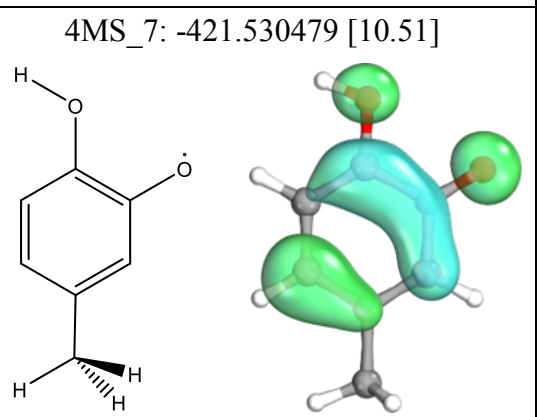
4MS_4: -421.545937 [0.81] 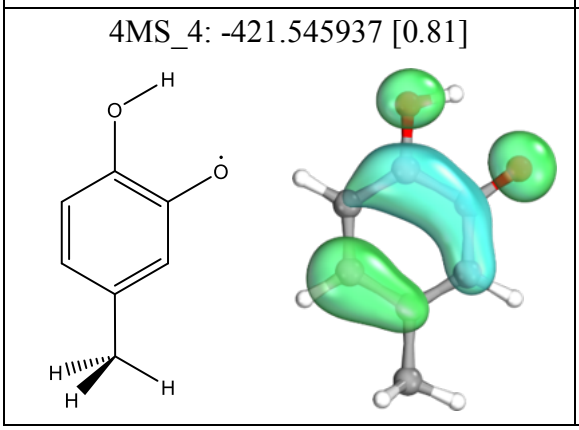	4MS_8: -421.544880 [1.48] 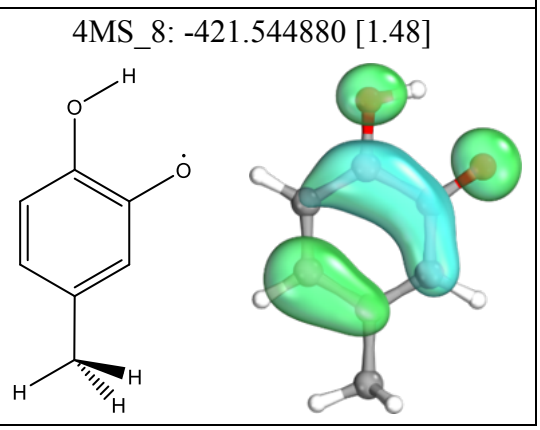

* Most stable conformation.

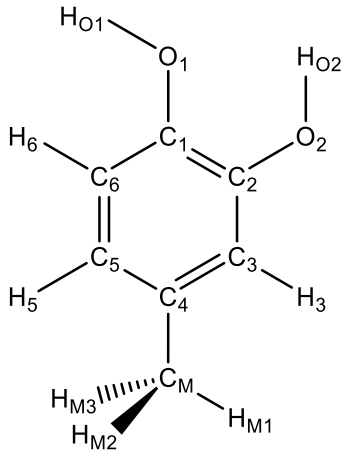

Scheme 2-SI. 4-metyl-catechol atoms numeration scheme.

Table 9-SI. B3LYP/G aug-cc-pVTZ spin density fraction on 4-methyl-semiquinone atoms. Atoms are named accordingly to Scheme 2-SI. The most stable conformation has been indicated with an asterisk, while the atom bearing the larger spin density fraction of each conformation has been highlighted in bold.

	Conformation							
Atom	**4MS_1***	**4MS_2**	**4MS_3**	**4MS_4**	**4MS_5**	**4MS_6**	**4MS_7**	**4MS_8**
C_1	0.083	0.052	0.206	0.207	0.082	0.050	0.194	0.199
C_2	0.183	0.187	0.046	0.076	0.169	0.171	0.046	0.076
C_3	-0.033	-0.036	0.126	0.093	-0.036	-0.039	0.143	0.106
C_4	0.200	0.211	-0.006	0.020	0.207	0.216	-0.008	0.019
C_5	0.024	-0.004	0.234	0.222	0.021	-0.005	0.228	0.218
C_6	0.113	0.138	-0.032	-0.026	0.130	0.157	-0.034	-0.027
O_1	**0.298**	**0.330**	0.085	0.098	**0.301**	**0.332**	0.080	0.093
O_2	0.083	0.075	**0.320**	**0.284**	0.077	0.068	**0.330**	**0.290**
C_M	0.016	0.017	0.001	0.003	0.016	0.017	0.000	0.002
H_{O1}	-	-	0.003	0.005	-	-	0.003	0.005
H_{O2}	0.005	0.003	-	-	0.004	0.003	-	-
H_3	-0.004	-0.005	0.006	0.004	-0.004	-0.004	0.007	0.005
H_5	0.000	-0.002	0.017	0.015	0.000	-0.001	0.017	0.015
H_6	0.005	0.007	-0.004	-0.003	0.006	0.008	-0.004	-0.004
H_{M1}	0.001	0.001	0.000	0.000	0.001	0.001	0.000	0.001
H_{M2}	0.013	0.013	-0.001	0.001	0.013	0.013	-0.001	0.001
H_{M3}	0.013	0.013	-0.001	0.001	0.013	0.013	-0.001	0.001
Total	1.000	1.000	1.000	1.000	1.000	1.000	1.000	1.000

Table 10-SI, part 1. Possible conformations of 3,4-dimethyl-semiquinone optimized at the B3LYP/G aug-cc-pVTZ level. For each conformer, the name, the formation energy (Hartrees) and the spin density are reported. The energy difference in kcal mol^{-1} with respect to the most stable conformation is reported into square brackets.

34MDS_1: -460.876572 [0.61] 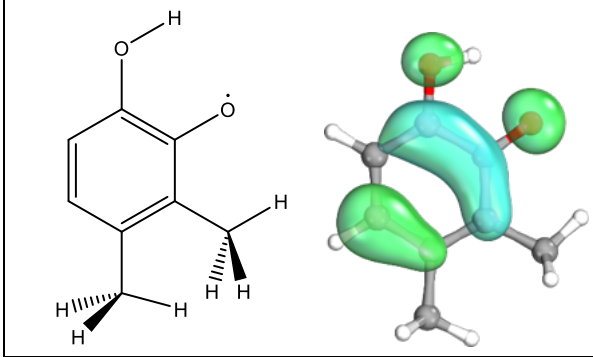	34MDS_5: -460.861947 [9.79] 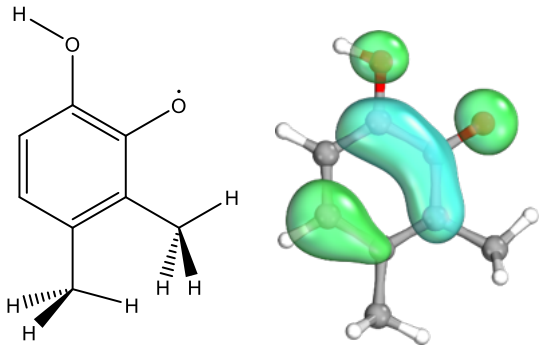
34MDS_2: -460.877547 [0.00]* 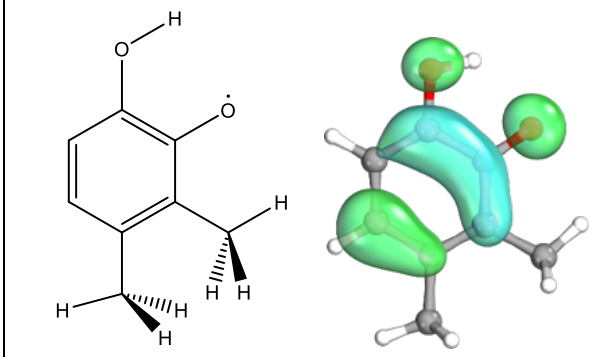	34MDS_6: -460.863164 [9.03] 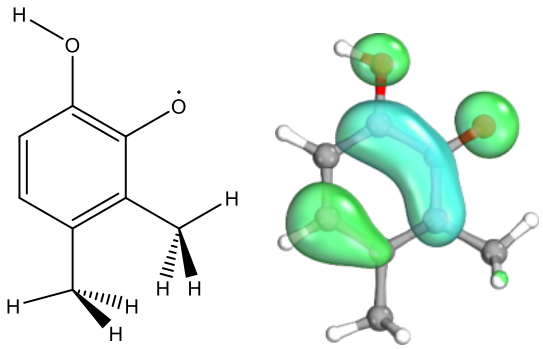
34MDS_3: -460.875981 [0.98] 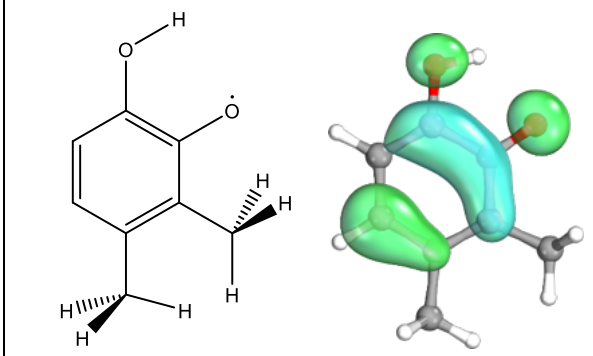	34MDS_7: -460.861356 [10.16] 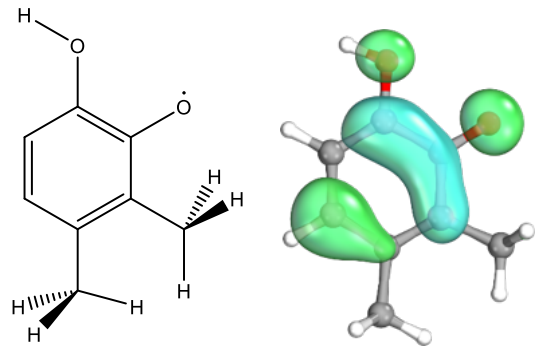
34MDS_4: -460.876985 [0.35] 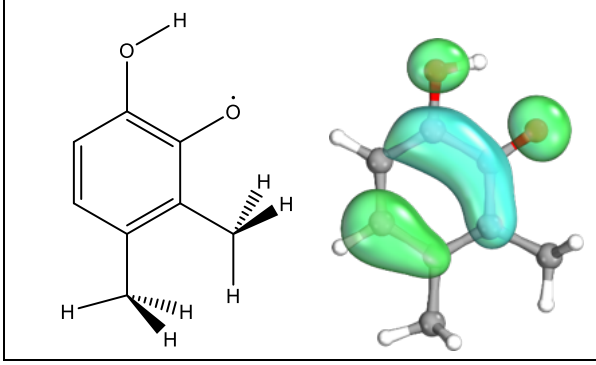	34MDS_8: -460.862621 [9.37] 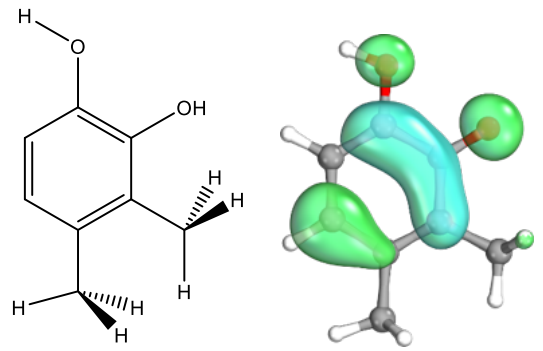

* Most stable conformation.

Table 10-SI, part 2. Possible conformations of 3,4-dimethyl-semiquinone optimized at the B3LYP/G aug-cc-pVTZ level. For each conformer, the name, the formation energy (Hartrees) and the spin density are reported. The energy difference in kcal mol^{-1} with respect to the most stable conformation is reported into square brackets.

34MDS_9: -460.876226 [0.83]	34MDS_13: -460.858768 [11.78]
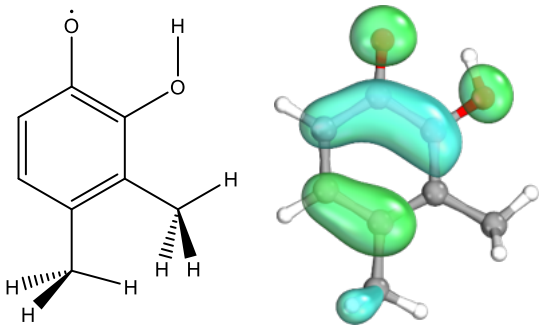	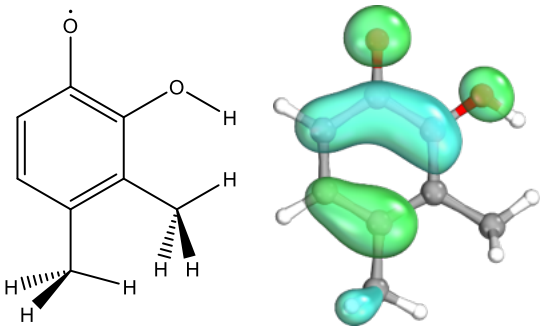
34MDS_10: -460.877374 [0.11]	34MDS_14: -460.860314 [10.81]
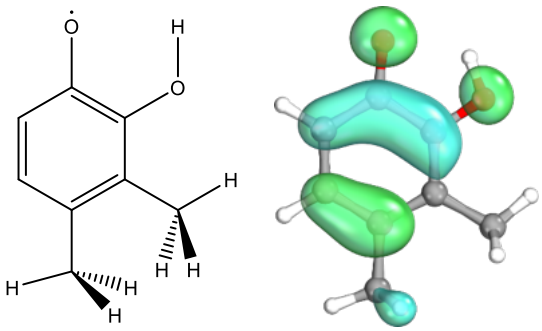	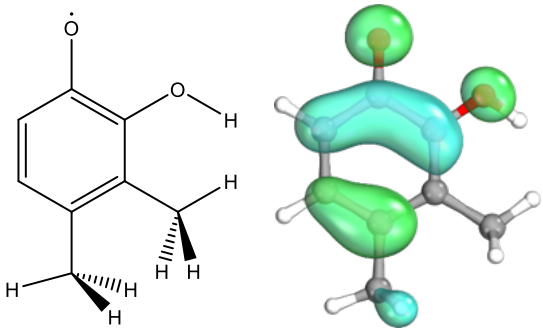
34MDS_11: -460.875441 [1.32]	34MDS_15: -460.859427 [11.37]
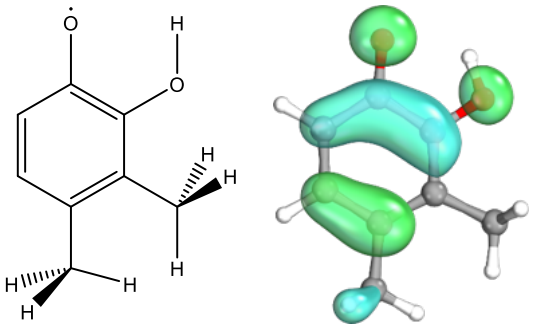	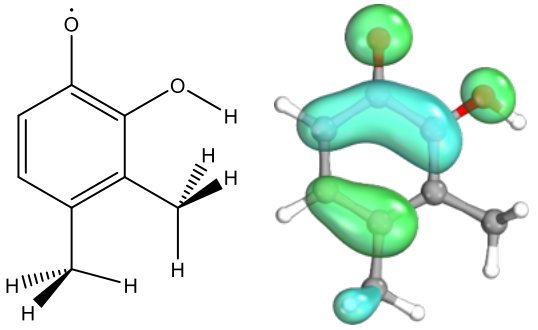
34MDS_12: -460.876781 [0.48]	34MDS_16: -460.861117 [10.31]
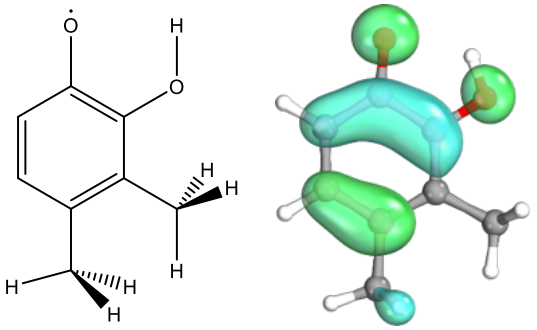	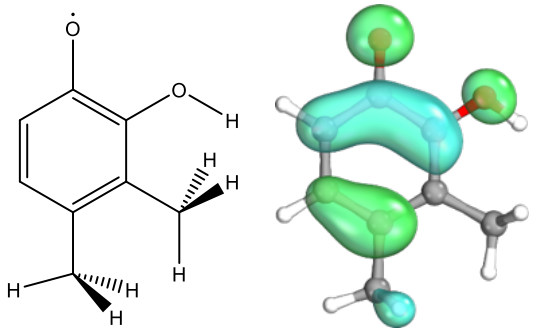

* Most stable conformation.

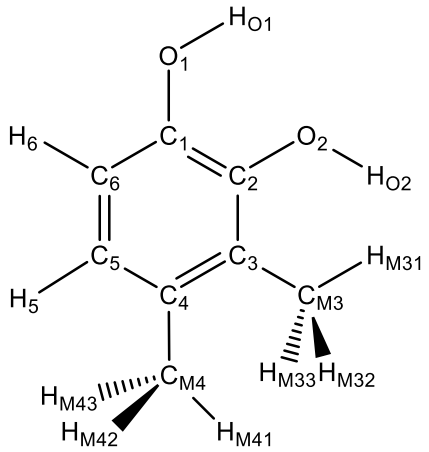

Scheme 3-SI. 3,4-dimethyl-catechol atoms numeration scheme.

Table 11-SI, part 1. B3LYP/G aug-cc-pVTZ spin density fraction on 3,4-dimethyl-semiquinone atoms. Atoms are named accordingly to Scheme 3-SI. The most stable conformation has been indicated with an asterisk, while the atom bearing the larger spin density fraction of each conformation has been highlighted in bold.

	Conformation							
Atom	**34DMS_1**	**34DMS_2***	**34DMS_3**	**34DMS_4**	**34DMS_5**	**34DMS_6**	**34DMS_7**	**34DMS_8**
C_1	0.199	0.190	0.202	0.192	0.198	0.187	0.203	0.190
C_2	0.089	0.089	0.089	0.089	0.058	0.059	0.058	0.059
C_3	0.103	0.116	0.098	0.113	0.135	0.150	0.128	0.145
C_4	0.005	0.003	0.008	0.005	-0.018	-0.019	-0.015	-0.017
C_5	0.220	0.216	0.224	0.219	0.230	0.223	0.234	0.227
C_6	-0.030	-0.031	-0.029	-0.031	-0.034	-0.035	-0.034	-0.035
O_1	0.092	0.088	0.093	0.089	0.080	0.075	0.082	0.078
O_2	**0.287**	**0.294**	**0.279**	**0.286**	**0.318**	**0.325**	**0.308**	**0.316**
C_{M3}	0.006	0.007	0.005	0.007	0.008	0.009	0.007	0.009
C_{M4}	0.002	0.001	0.003	0.001	0.000	-0.001	0.001	-0.001
H_{O1}	0.005	0.005	0.005	0.005	0.003	0.003	0.003	0.003
H_{O2}	-	-	-	-	-	-	-	-
H_5	0.015	0.015	0.015	0.016	0.017	0.016	0.017	0.018
H_6	-0.003	-0.004	-0.004	-0.004	-0.004	-0.004	-0.004	-0.004
H_{M31}	0.000	0.000	0.000	0.000	0.000	0.000	0.000	0.000
H_{M32}	0.005	0.005	0.005	0.006	0.006	0.008	0.007	0.008
H_{M33}	0.005	0.005	0.005	0.006	0.006	0.008	0.007	0.008
H_{M41}	0.000	0.001	0.000	0.001	0.000	0.000	0.000	0.000
H_{M42}	0.000	0.000	0.001	0.000	-0.001	-0.002	-0.001	-0.002
H_{M43}	0.000	0.000	0.001	0.000	-0.001	-0.002	-0.001	-0.002
Total	1.000	1.000	1.000	1.000	1.000	1.000	1.000	1.000

Table 11-SI, part 2. B3LYP/G aug-cc-pVTZ spin density fraction on 3,4-dimethyl-semiquinone atoms. Atoms are named accordingly to Scheme 3-SI. The most stable conformation has been indicated with an asterisk, while the atom bearing the larger spin density fraction of each conformation has been highlighted in bold.

	Conformation							
Atom	**34DMS_9**	**34DMS_10**	**34DMS_11**	**34DMS_12**	**34DMS_13**	**34DMS_14**	**34DMS_15**	**34DMS_16**
C_1	0.085	0.084	0.085	0.084	0.051	0.050	0.052	0.051
C_2	0.185	0.176	0.195	0.182	0.187	0.176	0.197	0.182
C_3	-0.032	-0.034	-0.031	-0.033	-0.036	-0.037	-0.035	-0.037
C_4	0.205	0.205	0.197	0.201	0.218	0.217	0.211	0.213
C_5	0.025	0.022	0.028	0.024	-0.004	-0.005	-0.002	-0.004
C_6	0.112	0.125	0.102	0.119	0.140	0.154	0.129	0.148
O_1	**0.292**	**0.297**	**0.293**	**0.299**	**0.324**	**0.330**	**0.327**	**0.332**
O_2	0.083	0.078	0.087	0.081	0.075	0.070	0.079	0.073
C_{M3}	-0.003	-0.003	-0.003	-0.004	-0.003	-0.004	-0.003	-0.003
C_{M5}	0.017	0.017	0.017	0.016	0.018	0.017	0.017	0.017
H_{O1}	-	-	-	-	-	-	-	-
H_{O2}	0.005	0.005	0.005	0.004	0.003	0.003	0.003	0.003
H_5	0.000	0.001	0.000	0.001	-0.002	-0.001	-0.002	-0.001
H_6	0.005	0.006	0.004	0.005	0.007	0.008	0.006	0.007
H_{M31}	0.000	0.000	0.000	0.000	-0.001	-0.001	0.000	0.000
H_{M32}	-0.003	-0.003	-0.003	-0.003	-0.003	-0.003	-0.003	-0.004
H_{M33}	-0.003	-0.003	-0.003	-0.003	-0.003	-0.003	-0.003	-0.004
H_{M51}	0.001	0.001	0.001	0.001	0.001	0.001	0.001	0.001
H_{M52}	0.013	0.013	0.013	0.013	0.014	0.014	0.013	0.013
H_{M53}	0.013	0.013	0.013	0.013	0.014	0.014	0.013	0.013
Total	1.000	1.000	1.000	1.000	1.000	1.000	1.000	1.000

Table 12-SI. Possible conformations of 3,6-dimethyl-semiquinone optimized at the B3LYP/G aug-cc-pVTZ level. For each conformer, the name, the formation energy (Hartrees) and the spin density are reported. The energy difference in kcal mol^{-1} with respect to the most stable conformation is reported into square brackets.

36DMS_1: -460.877841 [1.53] 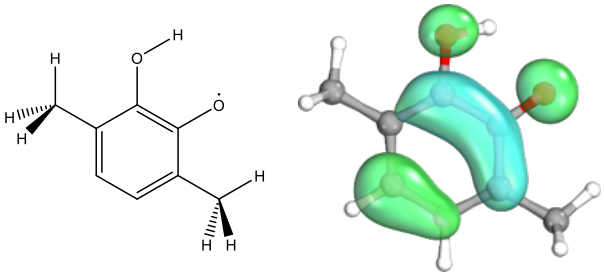	36DMS_5: -460.861608 [11.72] 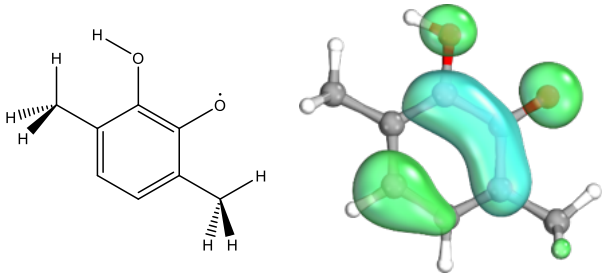
36DMS_2: -460.878911 [0.86] 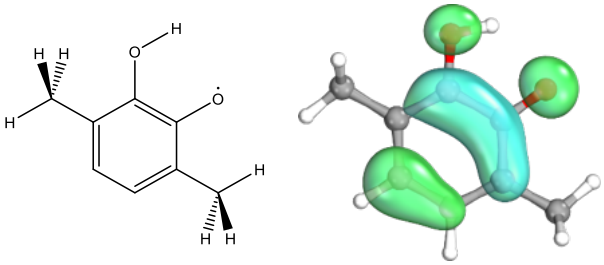	36DMS_6: -460.863749 [10.38] 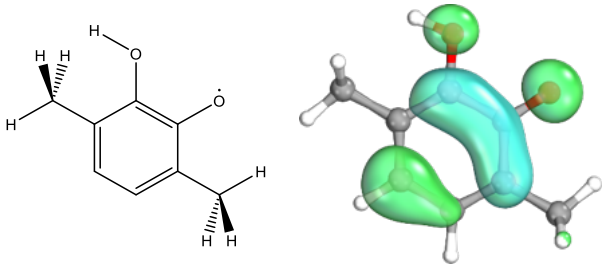
36DMS_3: -460.879178 [0.70] 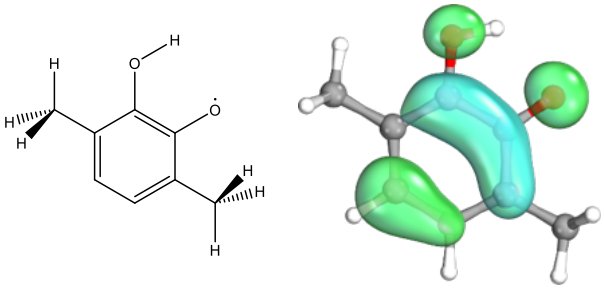	36DMS_7: -460.862951 [10.88] 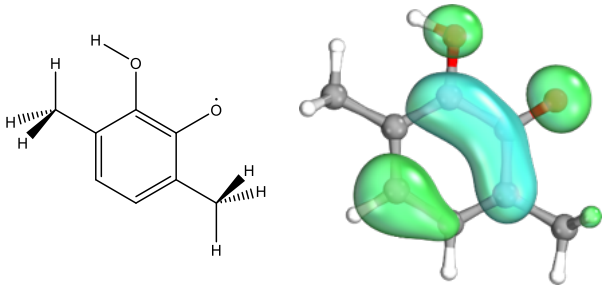
36DMS_4: -460.880287 [0.00]* 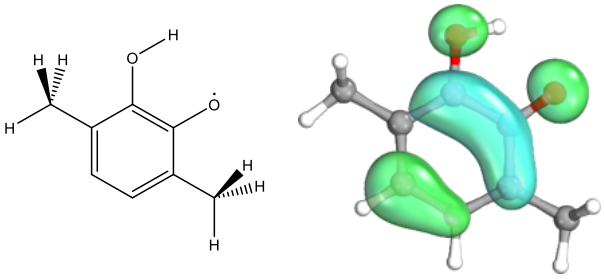	36DMS_8: -460.865133 [9.51] 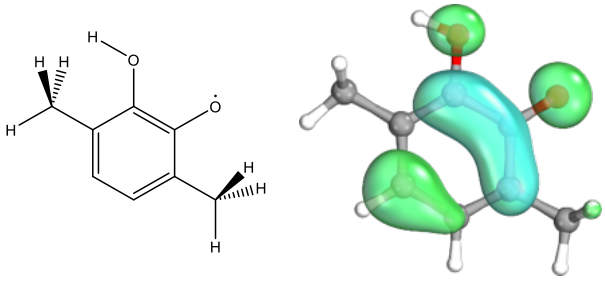

* Most stable conformation.

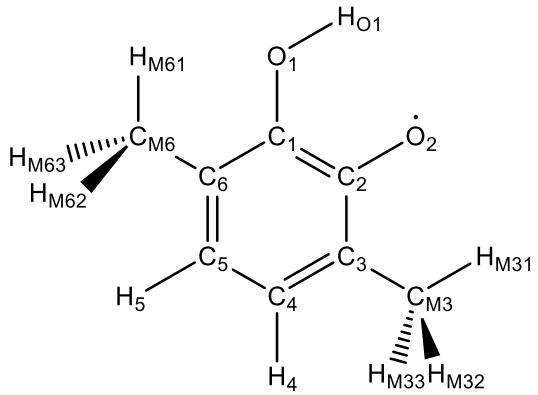

Scheme 4-SI. 3,6-dimethyl-semiquinone atoms numeration scheme.

Table 13-SI. B3LYP/G aug-cc-pVTZ spin density fraction on 3,6-dimethyl-semiquinone atoms. Atoms are named accordingly to Scheme 4-SI. The most stable conformation has been indicated with an asterisk, while the atom bearing the larger spin density fraction of each conformation has been highlighted in bold.

	Conformation							
Atom	**36DMS_1**	**36DMS_2**	**36DMS_3**	**36DMS_4***	**36DMS_5**	**36DMS_6**	**36DMS_7**	**36DMS_8**
C_1	0.177	0.189	0.182	0.194	0.173	0.186	0.180	0.193
C_2	0.092	0.092	0.092	0.093	0.059	0.059	0.058	0.059
C_3	0.139	0.127	0.131	0.119	0.170	0.157	0.160	0.147
C_4	-0.003	0.000	0.001	0.004	-0.023	-0.022	-0.019	-0.018
C_5	0.213	0.203	0.217	0.206	0.223	0.214	0.229	0.219
C_6	-0.032	-0.030	-0.031	-0.029	-0.035	-0.034	-0.035	-0.033
O_1	0.080	0.086	0.083	0.089	0.070	0.075	0.074	0.079
O_2	**0.301**	**0.303**	**0.293**	**0.294**	**0.328**	**0.332**	**0.317**	**0.321**
C_{M3}	0.008	0.007	0.007	0.007	0.010	0.009	0.009	0.008
C_{M6}	-0.003	-0.003	-0.003	-0.003	-0.003	-0.003	-0.003	-0.003
H_{O1}	0.005	0.005	0.005	0.005	0.003	0.003	0.003	0.003
H_4	0.000	0.000	0.000	0.000	-0.002	-0.002	-0.002	-0.002
H_5	0.016	0.015	0.016	0.015	0.017	0.016	0.017	0.017
H_{M31}	0.000	0.000	0.000	0.000	0.000	0.000	0.000	0.000
H_{M32}	0.007	0.006	0.007	0.006	0.008	0.008	0.009	0.008
H_{M33}	0.007	0.006	0.007	0.006	0.008	0.008	0.009	0.008
H_{M61}	-0.001	0.000	-0.001	0.000	0.000	0.000	0.000	0.000
H_{M62}	-0.003	-0.003	-0.003	-0.003	-0.003	-0.003	-0.003	-0.003
H_{M63}	-0.003	-0.003	-0.003	-0.003	-0.003	-0.003	-0.003	-0.003
Total	1.000	1.000	1.000	1.000	1.000	1.000	1.000	1.000

Table 14-SI. Possible conformations of 4,5-dimethyl-semiquinone optimized at the B3LYP/G aug-cc-pVTZ level. For each conformer, the name, the formation energy (Hartrees) and the spin density are reported. The energy difference in kcal mol^{-1} with respect to the most stable conformation is reported into square brackets.

45DMS_1: -460.878107 [0.00]* 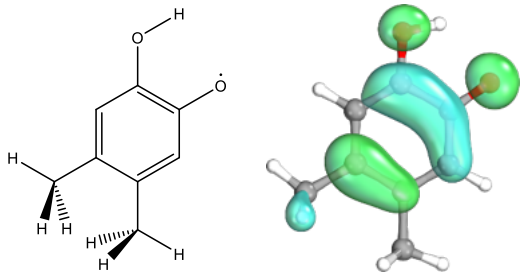	45DMS_5: -460.863542 [9.14] 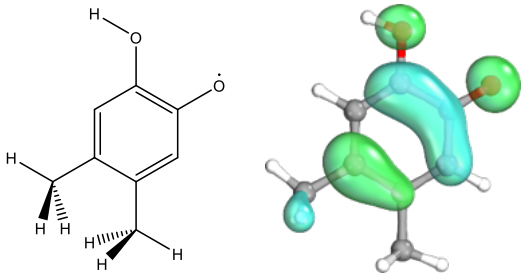
45DMS_2: -460.876134 [1.24] 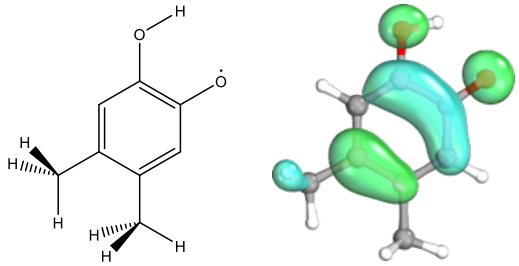	45DMS_6: -460.861714 [10.29] 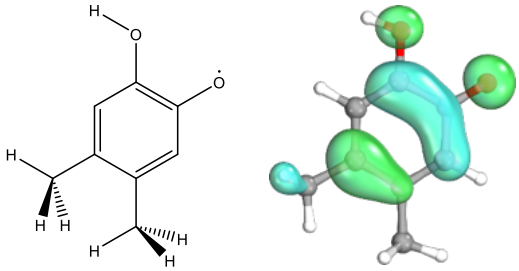
45DMS_3: -460.875595 [1.58] 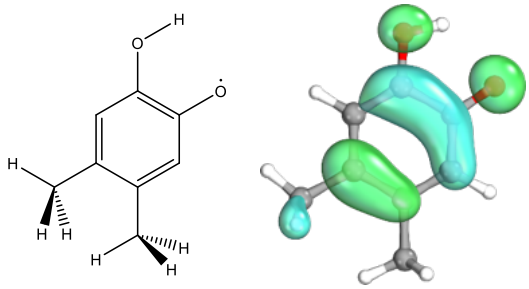	45DMS_7: -460.861151 [10.64] 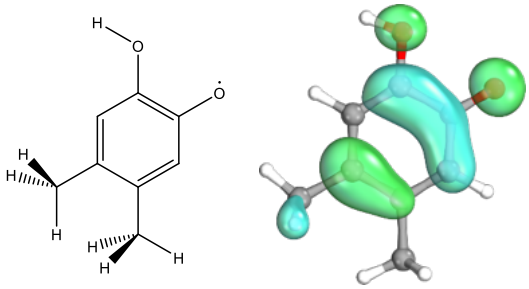
45DMS_4: -460.873021 [3.19] 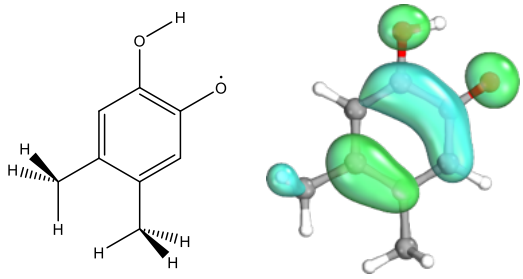	45DMS_8: -460.858834 [12.09] 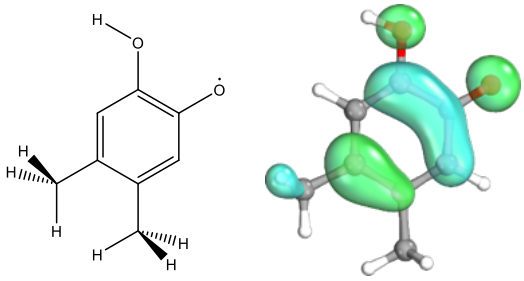

* Most stable conformation.

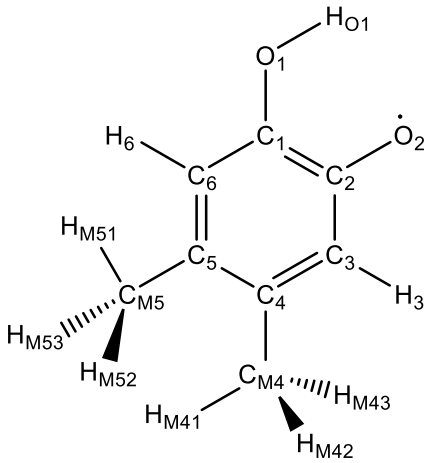

Scheme 5-SI. 4,5-dimethyl-semiquinone atoms numeration scheme.

Table 15-SI. B3LYP/G aug-cc-pVTZ spin density fraction on 4,5-dimethyl-semiquinone atoms. Atoms are named accordingly to Scheme 5-SI. The most stable conformation has been indicated with an asterisk, while the atom bearing the larger spin density fraction of each conformation has been highlighted in bold.

	Conformation							
Atom	**45DMS_1***	**45DMS_2**	**45DMS_3**	**45DMS_4**	**45DMS_5**	**45DMS_6**	**45DMS_7**	**45DMS_8**
C_1	0.192	0.180	0.187	0.171	0.194	0.180	0.187	0.169
C_2	0.081	0.080	0.080	0.079	0.051	0.050	0.051	0.049
C_3	0.097	0.108	0.104	0.121	0.126	0.139	0.136	0.155
C_4	0.026	0.024	0.026	0.023	-0.001	-0.002	-0.003	-0.005
C_5	0.211	0.221	0.210	0.220	0.220	0.229	0.218	0.226
C_6	-0.032	-0.035	-0.032	-0.036	-0.035	-0.038	-0.036	-0.039
O_1	0.087	0.082	0.085	0.078	0.077	0.072	0.075	0.067
O_2	**0.288**	**0.288**	**0.290**	**0.293**	**0.322**	**0.321**	**0.326**	**0.328**
C_{M4}	0.001	0.002	0.001	0.001	-0.001	0.000	-0.001	0.000
C_{M5}	0.016	0.016	0.016	0.017	0.017	0.017	0.017	0.017
H_{O1}	0.004	0.004	0.005	0.004	0.003	0.003	0.003	0.003
H_3	0.004	0.005	0.005	0.006	0.006	0.007	0.007	0.008
H_6	-0.004	-0.004	-0.004	-0.004	-0.004	-0.005	-0.005	-0.005
H_{M41}	0.000	0.000	0.000	0.000	0.000	0.000	0.000	0.000
H_{M42}	0.001	0.001	0.000	0.000	-0.001	-0.001	-0.001	-0.001
H_{M43}	0.001	0.001	0.000	0.000	-0.001	-0.001	-0.001	-0.001
H_{M51}	0.001	0.001	0.001	0.001	0.001	0.001	0.001	0.001
H_{M52}	0.013	0.013	0.013	0.013	0.013	0.014	0.013	0.014
H_{M53}	0.013	0.013	0.013	0.013	0.013	0.014	0.013	0.014
Total	1.000	1.000	1.000	1.000	1.000	1.000	1.000	1.000

Table 16-SI, part 1. Possible conformations of 3,5-dimethyl-semiquinone optimized at the B3LYP/G aug-cc-pVTZ level. For each conformer, the name, the formation energy (Hartrees) and the spin density are reported. The energy difference in kcal mol^{-1} with respect to the most stable conformation is reported into square brackets.

35DMS_1: -460.880135 [0.88] 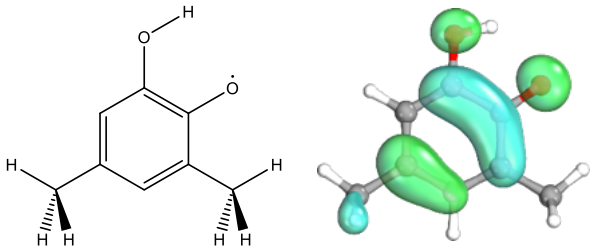	35DMS_5: -460.865663 [9.97] 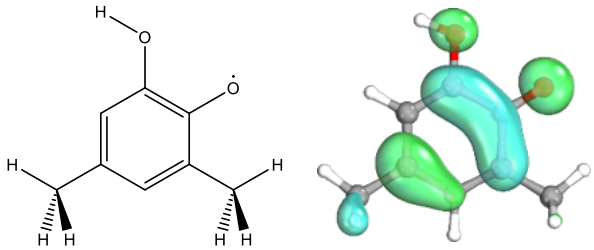
35DMS_2: -460.879828 [1.08] 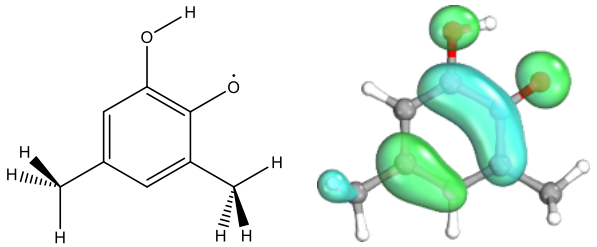	35DMS_6: -460.865502 [10.07] 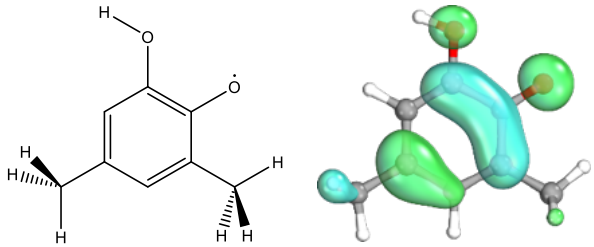
35DMS_3: -460.881543 [0.00]* 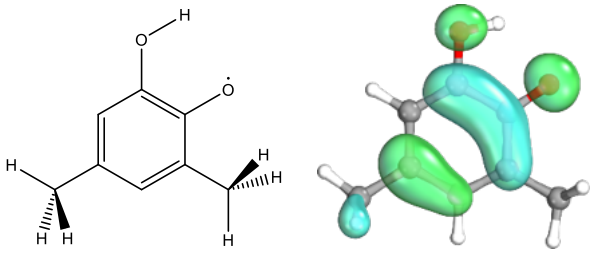	35DMS_7: -460.867112 [9.06] 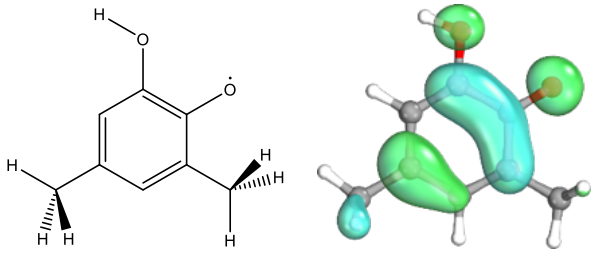
35DMS_4: -460.881144 [0.25] 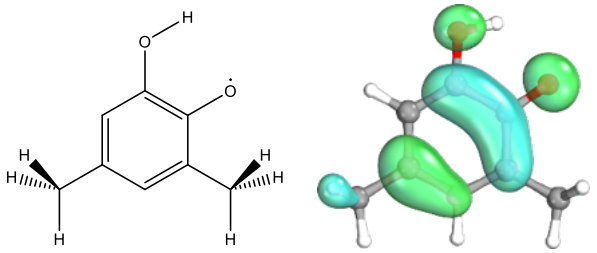	35DMS_8: -460.866843 [9.22] 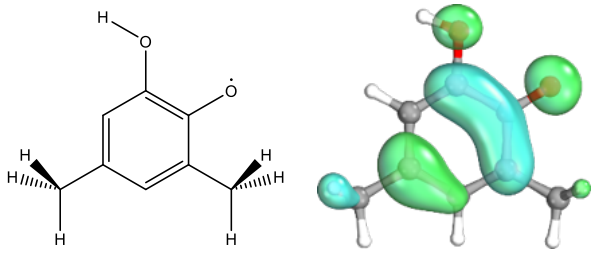

* Most stable conformation.

Table 16-SI, part 2. Possible conformations of 3,5-dimethyl-semiquinone optimized at the B3LYP/G aug-cc-pVTZ level. For each conformer, the name, the formation energy (Hartrees) and the spin density are reported. The energy difference in kcal mol^{-1} with respect to the most stable conformation is reported into square brackets.

35DMS_9: -460.877227 [2.71]	35DMS_13: -460.860485 [13.21]
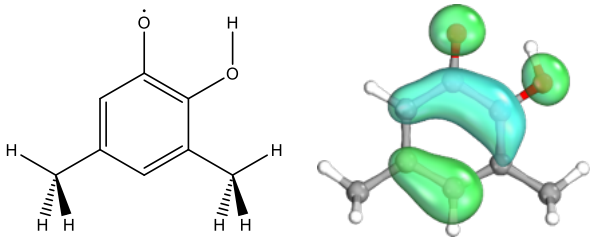	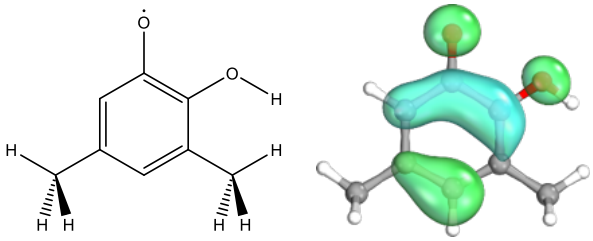
35DMS_10: -460.876163 [3.38]	35DMS_14: -460.859612 [13.76]
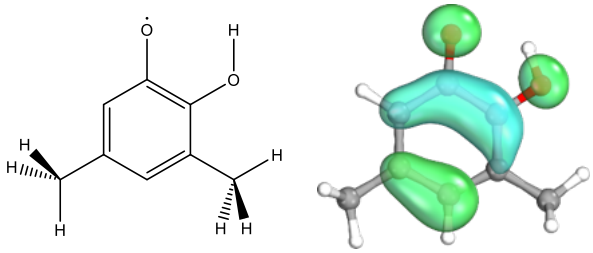	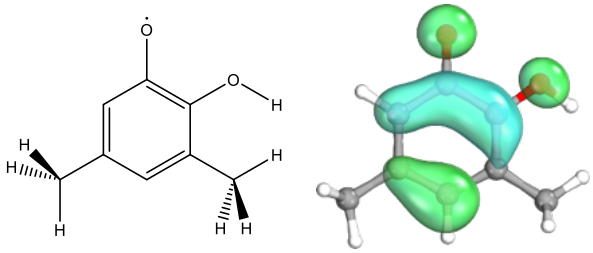
35DMS_11: -460.878427 [1.96]	35DMS_15: -460.862743 [11.80]
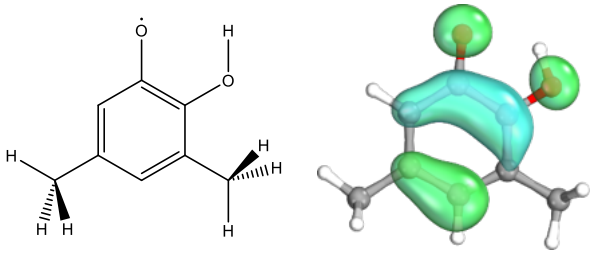	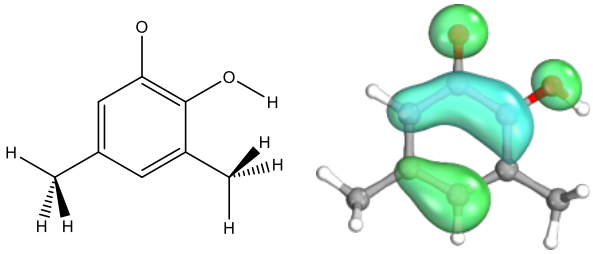
35DMS_12: -460.877281 [2.67]	35DMS_16: -460.861761 [12.41]
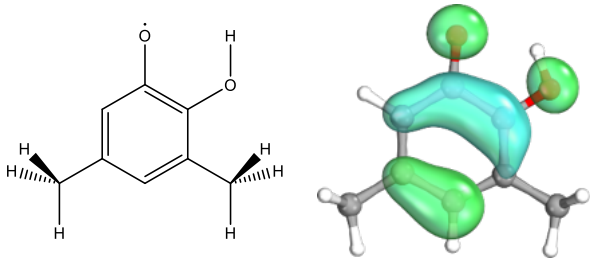	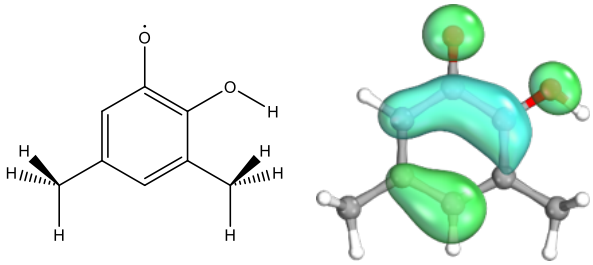

* Most stable conformation.

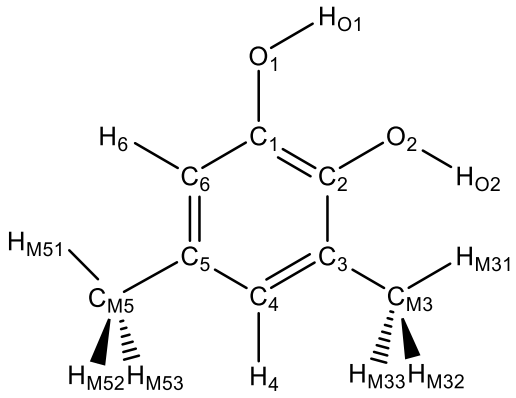

Scheme 6-SI. 3,5-dimethyl-catechol atoms numeration scheme.

Table 17-SI, part 1. B3LYP/G aug-cc-pVTZ spin density fraction on 3,5-dimethyl-semiquinone atoms. Atoms are named accordingly to Scheme 6-SI. The most stable conformation has been indicated with an asterisk, while the atom bearing the larger spin density fraction of each conformation has been highlighted in bold.

	Conformation							
Atom	**35DMS_1**	**35DMS_2**	**35DMS_3***	**35DMS_4**	**35DMS_5**	**35DMS_6**	**35DMS_7**	**35DMS_8**
C_1	0.175	0.159	0.180	0.165	0.179	0.162	0.185	0.169
C_2	0.096	0.095	0.096	0.095	0.064	0.063	0.064	0.063
C_3	0.121	0.140	0.114	0.132	0.145	0.165	0.136	0.155
C_4	0.008	0.004	0.010	0.007	-0.016	-0.017	-0.012	-0.014
C_5	0.196	0.200	0.200	0.204	0.204	0.207	0.209	0.212
C_6	-0.034	-0.037	-0.034	-0.037	-0.036	-0.038	-0.036	-0.038
O_1	0.078	0.071	0.081	0.074	0.070	0.063	0.073	0.066
O_2	**0.300**	**0.303**	**0.293**	**0.295**	**0.328**	**0.330**	**0.318**	**0.319**
C_{M3}	0.006	0.008	0.006	0.008	0.008	0.010	0.008	0.009
C_{M5}	0.016	0.016	0.016	0.016	0.016	0.016	0.017	0.017
H_{O1}	0.004	0.004	0.004	0.004	0.003	0.002	0.003	0.003
H_{O2}	-	-	-	-	-	-	-	-
H_4	-0.001	0.000	-0.001	0.000	-0.002	-0.002	-0.002	-0.002
H_6	-0.004	-0.004	-0.004	-0.004	-0.004	-0.004	-0.004	-0.005
H_{M31}	0.000	0.000	0.000	0.000	0.000	0.000	0.000	0.000
H_{M32}	0.006	0.007	0.006	0.007	0.007	0.008	0.007	0.008
H_{M33}	0.006	0.007	0.006	0.007	0.007	0.008	0.007	0.008
H_{M51}	0.001	0.001	0.001	0.001	0.001	0.001	0.001	0.001
H_{M52}	0.013	0.013	0.013	0.013	0.013	0.013	0.013	0.013
H_{M53}	0.013	0.013	0.013	0.013	0.013	0.013	0.013	0.013
Total	1.000	1.000	1.000	1.000	1.000	1.000	1.000	1.000

Table 17-SI, part 2. B3LYP/G aug-cc-pVTZ spin density fraction on 3,5-dimethyl-semiquinone atoms. Atoms are named accordingly to Scheme 6-SI. The most stable conformation has been indicated with an asterisk, while the atom bearing the larger spin density fraction of each conformation has been highlighted in bold.

	Conformation							
Atom	**35DMS_9**	**35DMS_10**	**35DMS_11**	**35DMS_12**	**35DMS_13**	**35DMS_14**	**35DMS_15**	**35DMS_16**
C_1	0.077	0.077	0.078	0.077	0.045	0.045	0.046	0.046
C_2	0.207	0.199	0.219	0.211	0.201	0.189	0.214	0.202
C_3	-0.024	-0.025	-0.021	-0.022	-0.031	-0.033	-0.029	-0.030
C_4	0.226	0.221	0.214	0.210	0.242	0.235	0.230	0.224
C_5	0.021	0.019	0.023	0.021	-0.007	-0.009	-0.005	-0.008
C_6	0.095	0.109	0.085	0.097	0.133	0.151	0.121	0.138
O_1	**0.279**	**0.287**	**0.280**	**0.287**	**0.316**	**0.326**	**0.319**	**0.328**
O_2	0.096	0.092	0.100	0.097	0.083	0.078	0.088	0.083
C_{M3}	-0.002	-0.002	-0.002	-0.002	-0.003	-0.003	-0.003	-0.003
C_{M5}	0.003	0.002	0.004	0.002	0.001	0.000	0.001	0.000
H_{O1}	-	-	-	-	-	-	-	-
H_{O2}	0.005	0.005	0.005	0.005	0.003	0.003	0.003	0.003
H_4	0.016	0.016	0.015	0.016	0.018	0.018	0.017	0.017
H_6	0.004	0.005	0.004	0.004	0.007	0.008	0.006	0.007
H_{M31}	0.000	0.000	0.000	0.000	0.000	-0.001	0.000	0.000
H_{M32}	-0.002	-0.003	-0.003	-0.003	-0.003	-0.003	-0.003	-0.003
H_{M33}	-0.002	-0.003	-0.003	-0.003	-0.003	-0.003	-0.003	-0.003
H_{M51}	-0.001	0.001	0.000	0.001	0.000	0.001	0.000	0.001
H_{M52}	0.001	0.000	0.001	0.001	-0.001	-0.001	-0.001	-0.001
H_{M53}	0.001	0.000	0.001	0.001	-0.001	-0.001	-0.001	-0.001
Total	1.000	1.000	1.000	1.000	1.000	1.000	1.000	1.000

Table 18-SI. B3LYP/G aug-cc-pVTZ formation energies in Hartree of the substituted catechols considered in this work. For each substituted catechol, the energy difference (ΔE) in kcal/mol with respect to the most stable intermediate is also reported.

Intermediate	**Formation energy (Hartree)**	**ΔE (kcal/mol)**
3MC_int4_open	-860.274140	5.0
3MC_int4_close	-860.276797	3.3
3MC_int5_open	-860.276568	3.5
3MC_int5_close	-860.278837	2.0
3MC_int6_open	-860.278787	2.1
3MC_int6_close	-860.282070	0.0
4MC_int3_open	-860.276598	3.6
4MC_int3_close	-860.277416	3.1
4MC_int5_open	-860.276200	3.8
4MC_int5_close	-860.279452	1.8
4MC_int6_open	-860.277969	2.7
4MC_int6_close	-860.282288	0.0
34DMC_int5_open	-899.603901	4.5
34DMC_int5_close	-899.607184	2.5
34DMC_int6_open	-899.607872	2.0
34DMC_int6_close	-899.611094	0.0
35DMC_int4_open	-899.606144	1.9
35DMC_int4_close	-899.608627	0.3
35DMC_int6_open	-899.607951	0.7
35DMC_int6_close	-899.609134	0.0
45DMC_int3_open	-899.604405	3.4
45DMC_int3_close	-899.609847	0.0
36DMC_int4_open	-899.605817	1.5
36DMC_int4_close	-899.608233	0.0

Table 19-SI Energy variations (in kcal/mol) along the relaxed surface scan

Starting catechol	ΔE (max – separated molecules) (kcal/mol)	ΔE (intermediate – max) (kcal/mol)
CAT[11]	9.5	-0.3
3MC	7.2	-0.3
4MC	8.1	-0.4
3,4DMC	7.7	-0.3
3,5DMC	10.1	-0.3
4,5DMC	7.5	-0.1
3,6DMC	10.4	-0.2

Figure 1-SI. Bar plot showing the *per* residue RMSD of Cα atoms belonging to residues in α, β and γ subunits (colored in red, magenta and blue, respectively) of the crystal structures of SPU bound to **3MC**, **4MC**, **3,4DMC**, **3,5DMC**, **4,5DMC**, and **3,6DMC** (PDB codes 6ZNY, 6ZNZ, 6ZO0, 6ZO1, 6ZO2 and 6ZO3) calculated with respect to the native enzyme (PDB code 4CEU) [10].

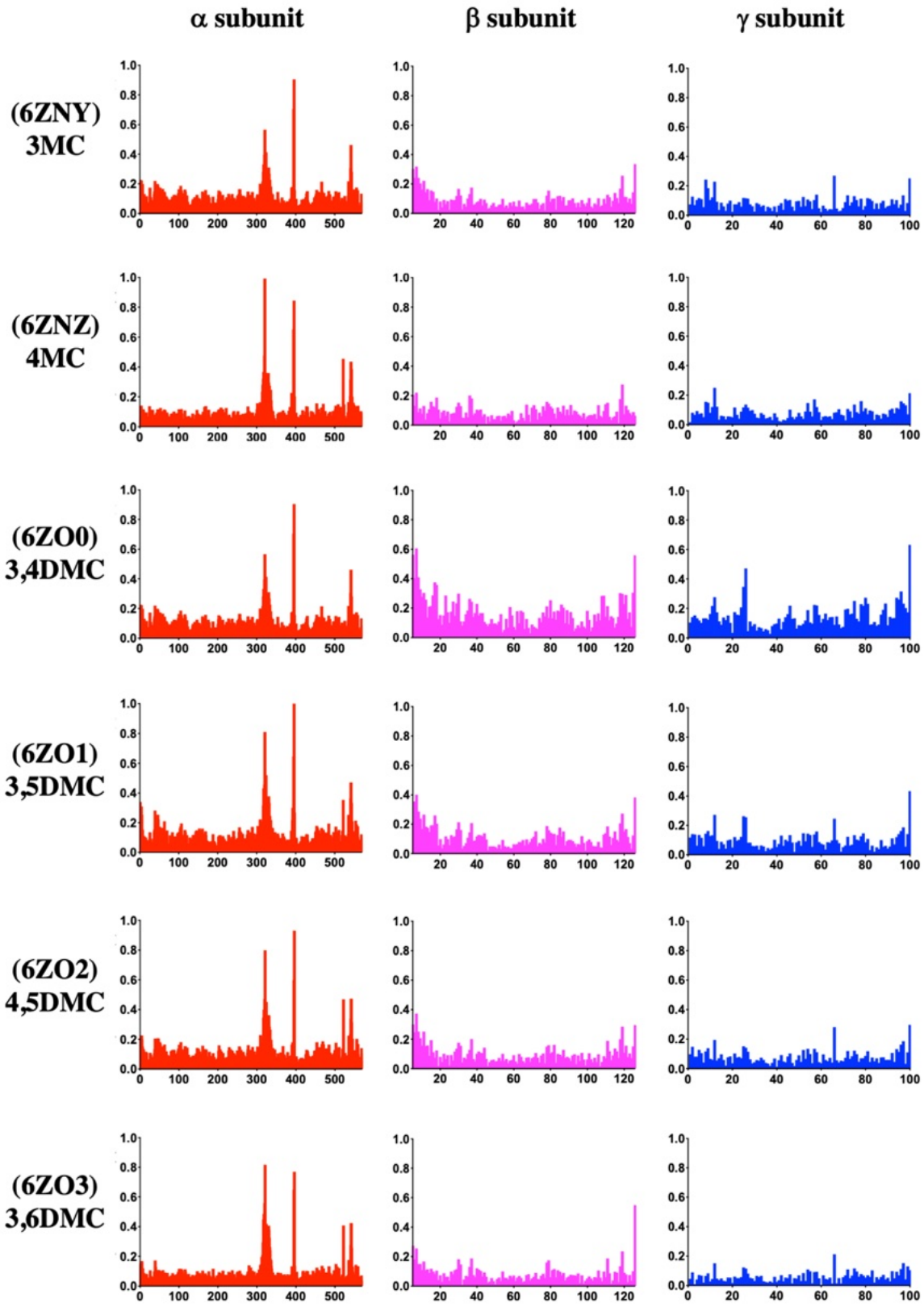

Figure 2-SI. Bar plot showing the *per* residue RMSD of Cα atoms belonging to residues in α, β and γ subunits (colored in black, purple and orange, respectively) of the crystal structures of SPU bound to **3MC**, **4MC**, **3,4DMC**, **3,5DMC**, **4,5DMC**, and **3,6DMC** (PDB codes 6ZNY, 6ZNZ, 6ZO0, 6ZO1, 6ZO2 and 6ZO3) calculated with respect to the structure of SPU bound to catechol (PDB code 5G4H) [11].

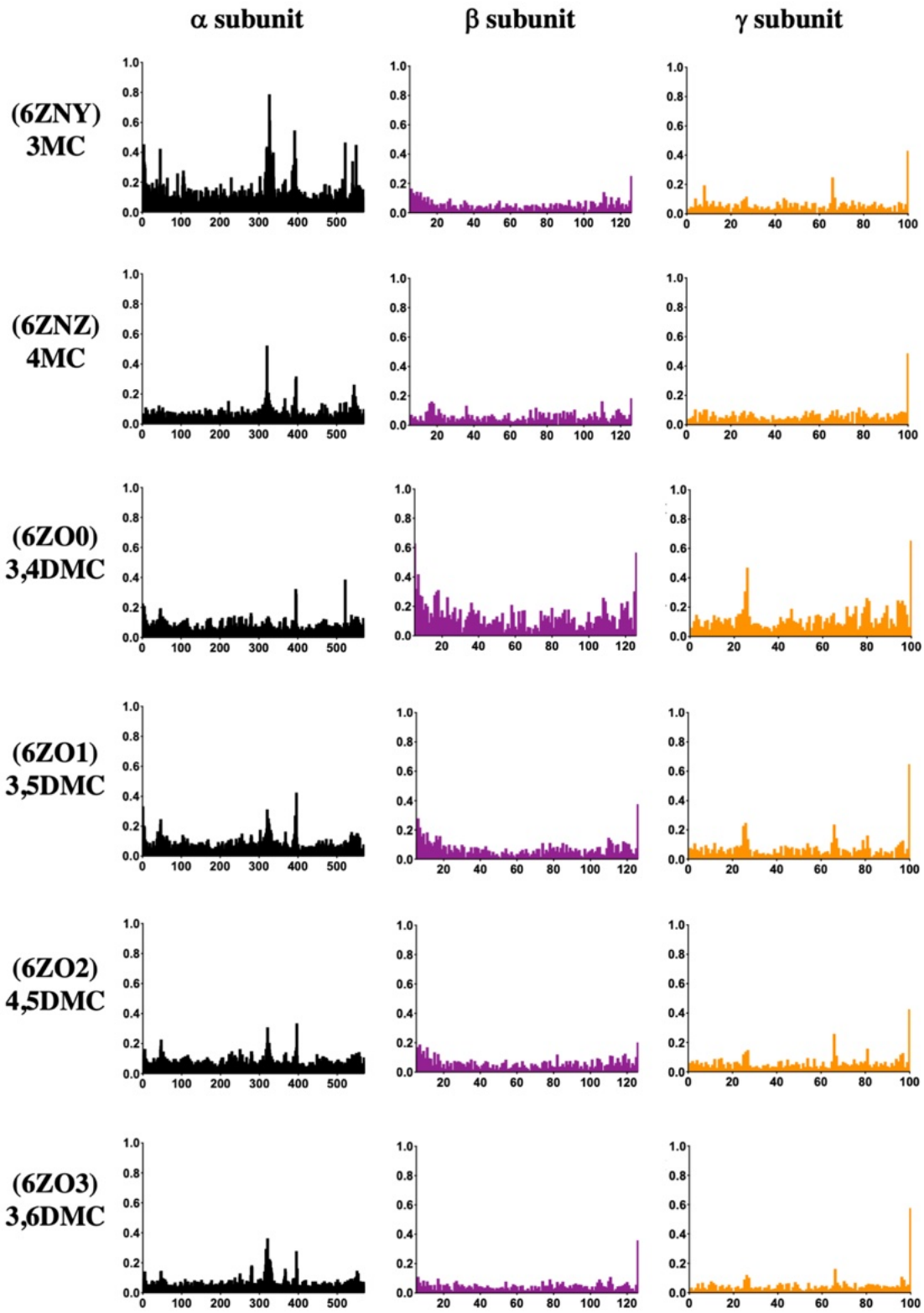

Figure 3-SI. Atomic models of the active site of SPU bound to **3MC** (A), **4MC** (B), **3,4DMC** (C), **3,5DMC** (D), **4,5DMC** (E), and **3,6DMC** (F) (PDB codes 6ZNY, 6ZNZ, 6ZO0, 6ZO1, 6ZO2 and 6ZO3). The carbon, nitrogen, oxygen, sulfur and nickel atoms are gray, blue, red, yellow and green, respectively. The unbiased F_o - F_c electron density map calculated with Fourier coefficients F_o - F_c and phases derived from the model before addition of the atoms corresponding to the ligands is shown colored blue and contoured at 3σ.

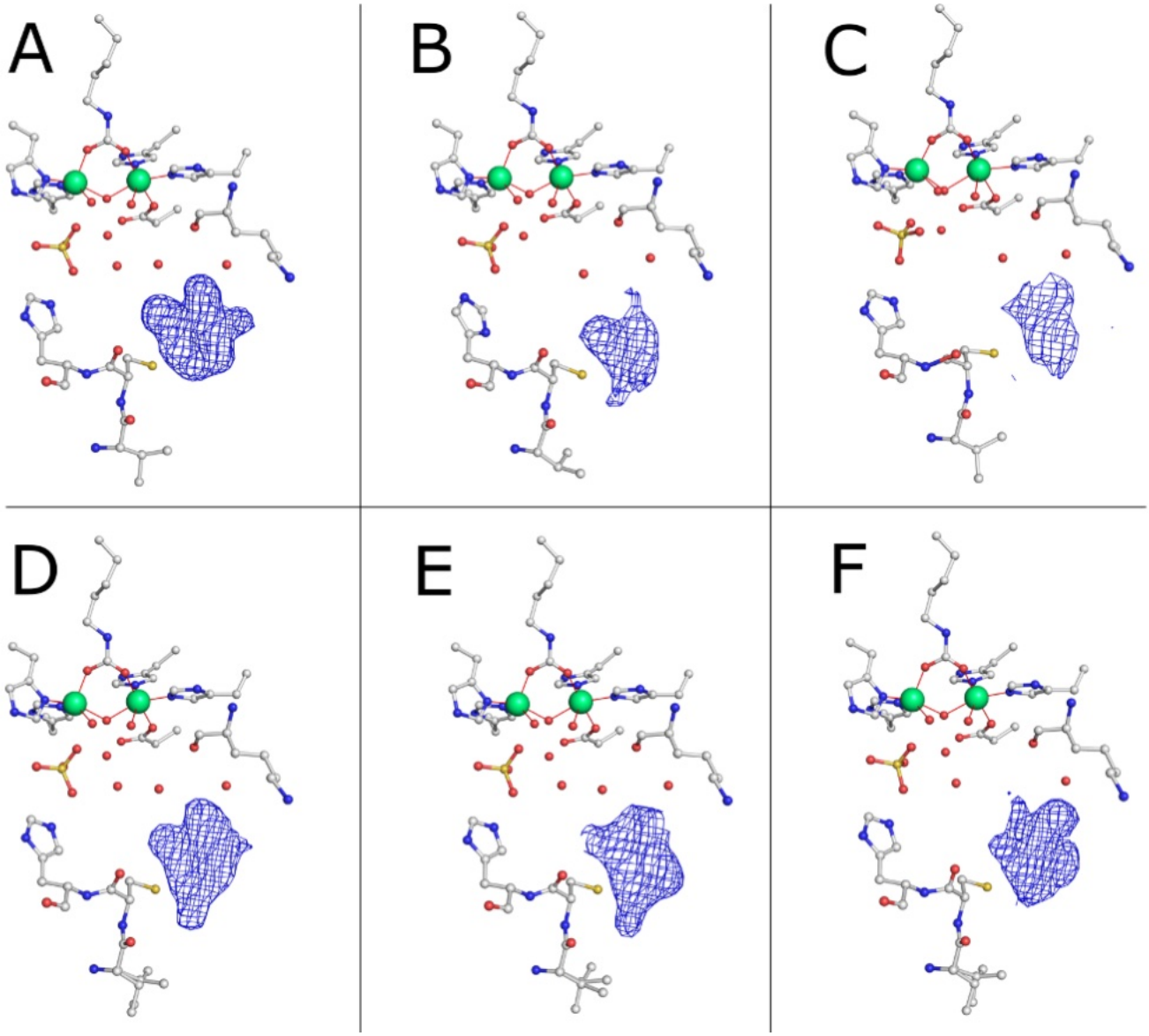

Figure 4-SI. Detail of the mobile flap region after the superimposition of all the X-ray structures determined in the present work together with the structure of SPU bound to catechol (PDB code 5G4H) [11]. The ribbons in the flap region, as well as the catechol derivatives, are colored according to the following scheme: CAT: orange; 3MC, blue; 4MC, green; 34DMC, light blue; 35DMC, red; 45DMC, light blue; 36DMC, purple. The side chain of αLys220* is in sticks colored according to atom type. The Ni(II) ions are shown as green spheres.

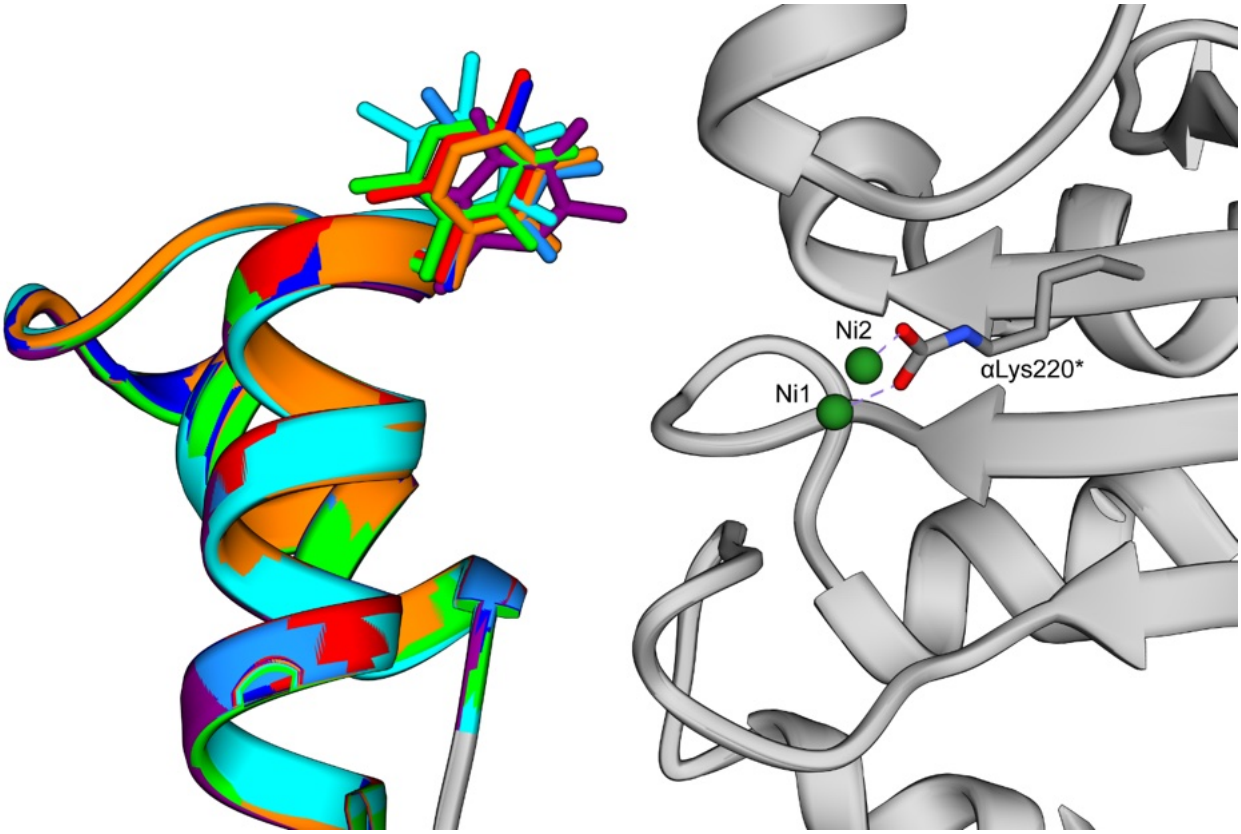

Figure 5-SI. Scheme of the H-bonding network (thin blue lines) in the vicinity of the SPU active site in the case of urease inactivation by **3MC** (PDB code 6ZNY). Spheres are drawn using the relative-atomic-radius values in CrystalMaker. The carbon, nitrogen, oxygen, sulphur, and nickel atoms are coloured grey, blue, red, yellow, and green, respectively.

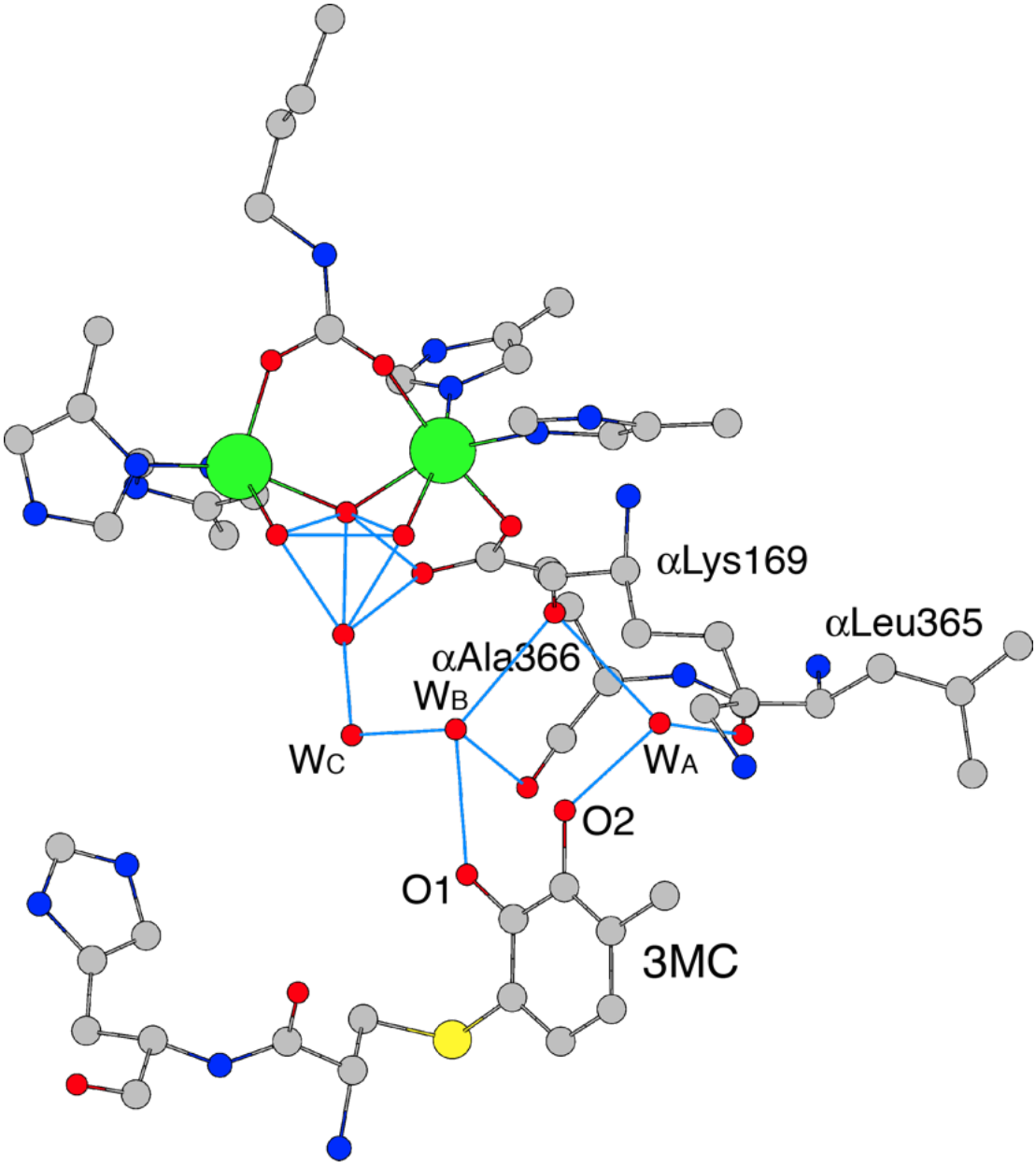

Figure 6-SI. B3LYP/G aug-cc-pVTZ spin density of the most stable conformation of 3-methyl-semiquinone (**A**), 4-methyl-semiquinone (**B**), 3-methoxy-semiquinone (**C**), 3,6-dimethyl-semiquinone (**D**), 4,5-dimethyl-semiquinone (**E**), and 3,5-dimethyl-semiquinone (**F**). The spin density fraction on the most relevant atoms has been indicated.

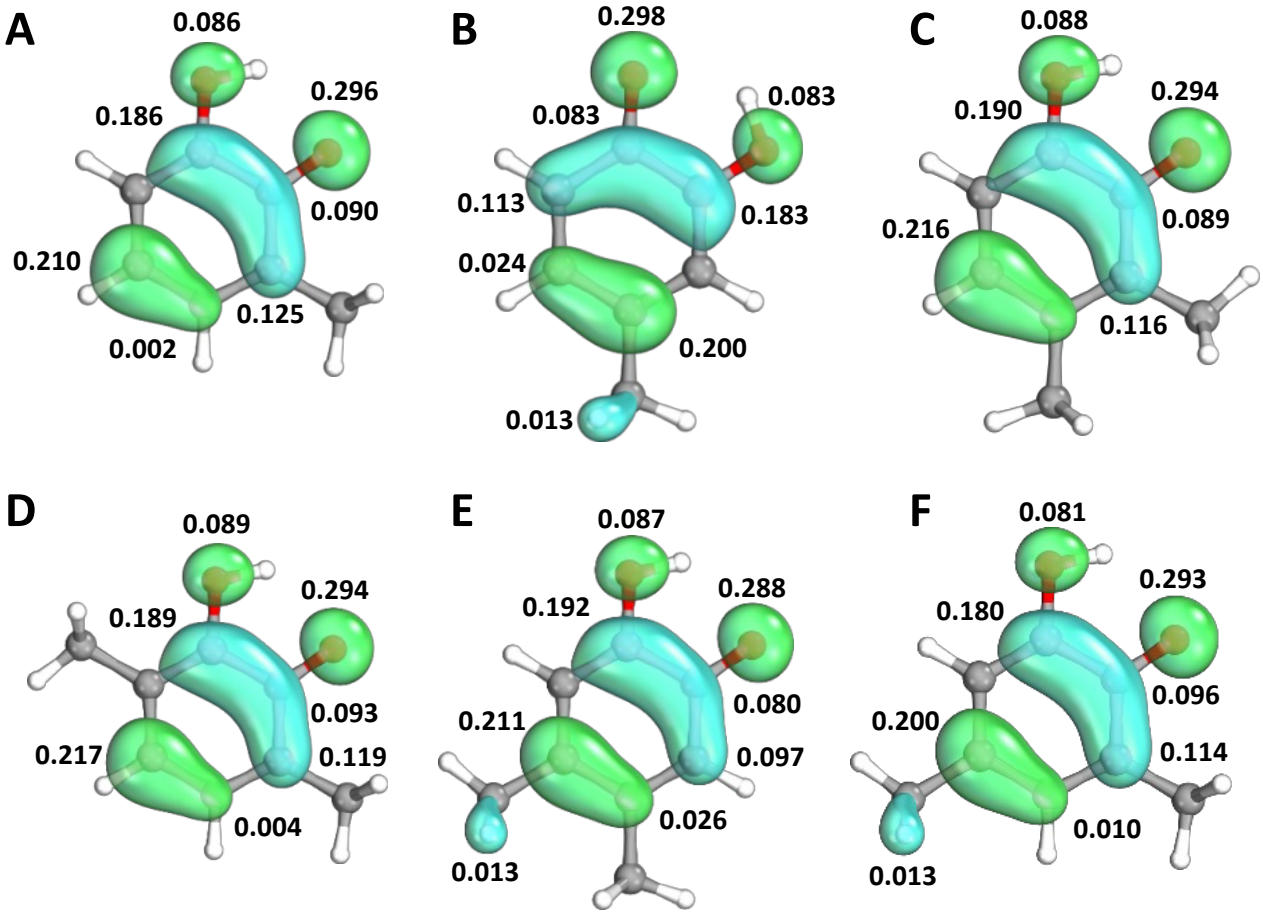

Figure 7-SI. B3LYP/G aug-cc-pVTZ optimized geometries and formation energies (in Hartree) of the reaction intermediate achieved starting from each of the monosubstituted catechols considered in this work. The carbon-sulfur distance (in Angstrom) is also reported. For each substituted catechol, the lowest energy structure has been highlighted with an asterisk.

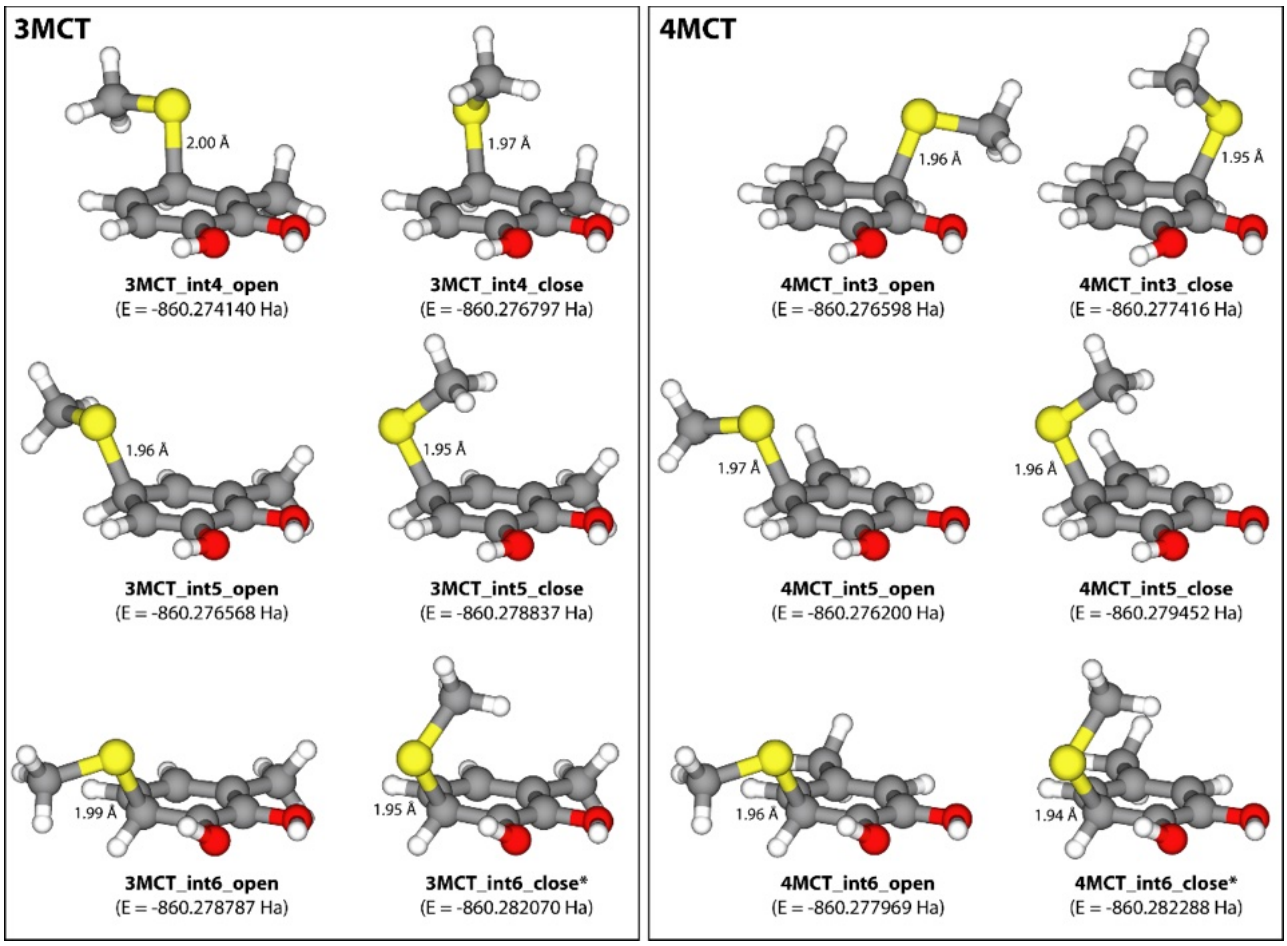

Figure 8-SI. B3LYP/G aug-cc-pVTZ optimized geometries and formation energies (in Hartree) of the reaction intermediate achieved starting from each of the disubstituted catechols considered in this work. The carbon-sulfur distance (in Angstrom) is also reported. For each substituted catechol, the lowest energy structure has been highlighted with an asterisk.

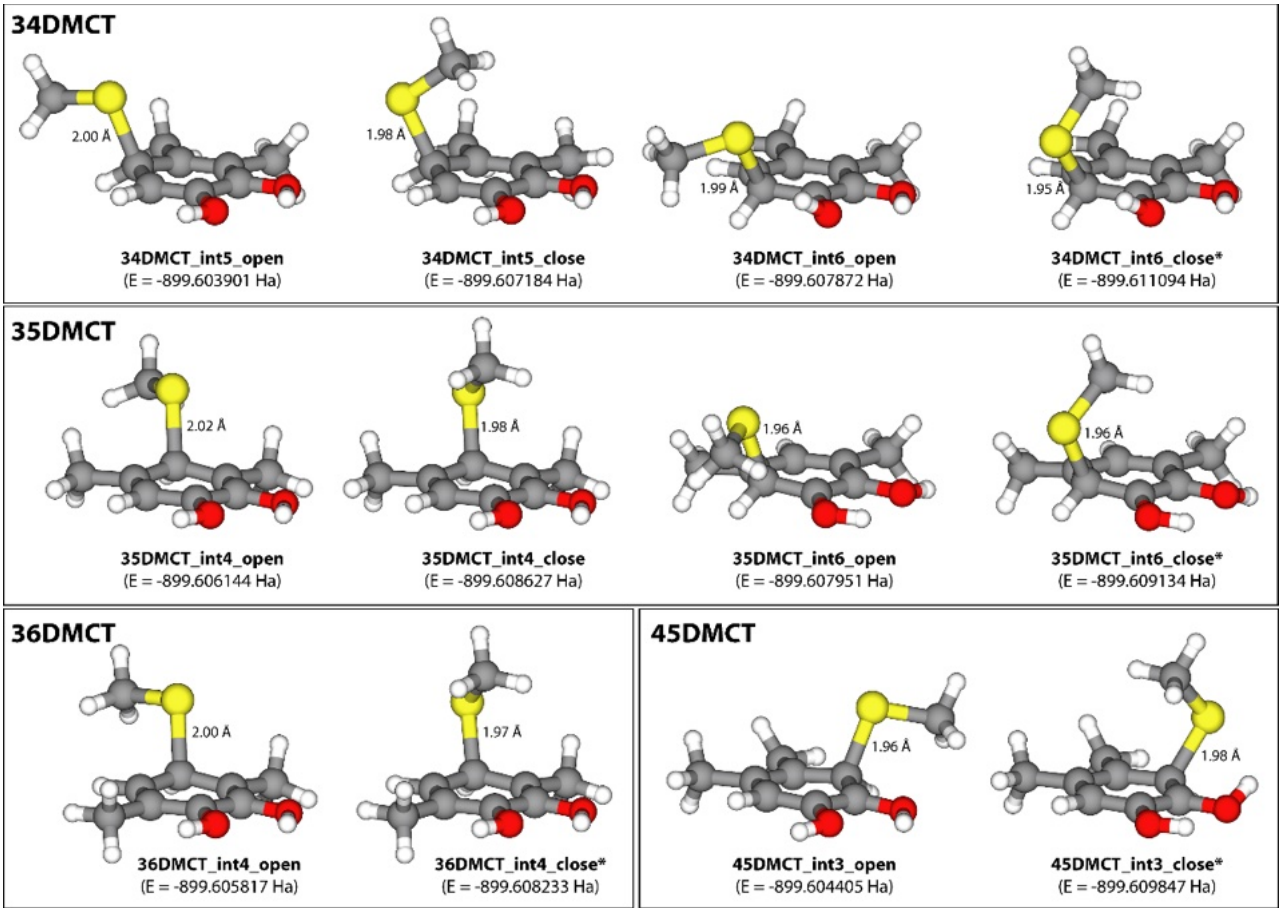

REFERENCES

[1] M. Iwatsu, D. Urabe, M. Inoue, *Heterocycles* **2010**, *82*, 491-504.

[2] A. Pezzella, L. Lista, A. Napolitano, M. d'Ischia, *Tetrahedron Lett.* **2005**, *46*, 3541-3544.

[3] D. D. Weller, E. P. Stirchak, *J. Org. Chem.* **1983**, *48*, 4873-4879.

[4] K. Shindo, R. Nakamura, A. Osawa, O. Kagami, K. Kanoh, K. Furukawa, N. Misawa, *J. Mol. Cat. B* **2005**, *35*, 134-141.

[5] C. Huang, N. Ghavtadze, B. Chattopadhyay, V. Gevorgyan, *J. Am. Chem. Soc.* **2011**, *133*, 17630-17633.

[6] M. Weiss, *Journal of Applied Crystallography* **2001**, *34*, 130-135.

[7] G. N. Murshudov, A. A. Vagin, E. J. Dodson, *Acta Crystallogr D Biol Crystallogr* **1997**, *53*, 240-255.

[8] D. W. Cruickshank, *Acta Crystallogr D Biol Crystallogr* **1999**, *55*, 583-601.

[9] M. D. Winn, C. C. Ballard, K. D. Cowtan, E. J. Dodson, P. Emsley, P. R. Evans, R. M. Keegan, E. B. Krissinel, A. G. Leslie, A. McCoy, S. J. McNicholas, G. N. Murshudov, N. S. Pannu, E. A. Potterton, H. R. Powell, R. J. Read, A. Vagin, K. S. Wilson, *Acta Crystallogr D Biol Crystallogr* **2011**, *67*, 235-242.

[10] S. Benini, M. Cianci, L. Mazzei, S. Ciurli, *J. Biol. Inorg. Chem.* **2014**, *19*, 1243-1261.

[11] L. Mazzei, M. Cianci, F. Musiani, G. Lente, M. Palombo, S. Ciurli, *J. Inorg. Biochem.* **2017**, *166*, 182-189.